Electronic structure of hydrogen-vacancy complexes in crystalline silicon: A theoretical study

Hongqi Xu
Department of Theoretical Physics, University of Lund, Sölvegatan 14A, S-22362 Lund, Sweden
(Received 25 April 1991; revised manuscript received 13 November 1991)

We report self-consistent calculations for the electronic structure of four complex defects, namely the monohydrogen-vacancy (VH), dihydrogen-vacancy (VH$_2$), trihydrogen-vacancy (VH$_3$), and quadrihydrogen-vacancy (VH$_4$) complexes, in crystalline silicon. The calculations are based on a semiempirical tight-binding theory. Each of the defects is described by a large repeated supercell. To overcome the difficulties in the treatment of large Hamiltonian matrices, we use the recursion method for computing the local densities of states and the localization of the defect states. We have also calculated numerically the wave functions of the fundamental gap states, which are, in turn, used to derive the hyperfine interaction parameters arising from the paramagnetic spin of the wave functions of the gap states for the complex defects. We have found that, in the VH$_4$ defect, the electrical activity is passivated by four hydrogen atoms, in agreement with early theoretical studies. For the defects VH, VH$_2$, and VH$_3$, we have found that the electrical activity is only partially passivated. We show that the nonhydrogenated silicon dangling orbitals are responsible for the remaining electrical activity. We also demonstrate that the Si-H bonding and antibonding states interact very weakly with the silicon dangling-bond states. Models accounting for the electronic structure of the four defects are presented. The effects of the symmetry-conserved distortions and the Jahn-Teller distortions on the electronic structure of the defects are examined. The calculations have been done in detail for the experimentally well-studied VH$_2$ defect. The results of these calculations agree well with recent experimental studies on this defect.

I. INTRODUCTION

The interactions between defects and hydrogen atoms in crystalline silicon are a phenomenon of great interest to both experimental and theoretical physicists.[1,2] It has been demonstrated that a large variety of defects in silicon can be passivated by exposure to hydrogen.[1,2] The microscopic structure of many shallow donor- and acceptor-hydrogen complexes has been well established.[2,3-11] The mechanisms of hydrogen passivation of many multivalent deep impurities have also been studied.[1,2] Here we are only concerned with hydrogen-vacancy complexes.

In a recent experimental work,[12] a hydrogen-vacancy-complex defect in silicon was studied by the optically detected magnetic resonance (ODMR) technique. The defect was identified as a neutral dihydrogen-vacancy complex in its lowest electronic excited state with a spin triplet. Two silicon dangling bonds were assumed to be passivated by the two hydrogen atoms. Two electrons with parallel spins, one in the bonding and the other one in the antibonding state of the two remaining silicon dangling bonds, are responsible for the ODMR spectra. Hydrogen-related defect complexes were also studied by deep level transient spectroscopy (DLTS).[13] In this study, an electron trap, labeled the Z center, was observed and assigned to the dihydrogen-vacancy-complex defect. The proposed electronic structure of the Z center is, however, different from that of Ref. 12. Three electrons were proposed to stay in the two electron states formed mainly from the two silicon dangling bonds in the defect. Among the three, two electrons with spin paired off were assumed to lie in the bonding state, while the remaining one was assumed to be in the antibonding state. This model shows that the dihydrogen-vacancy-complex defect observed from the DLTS spectra stays in a spin-singlet state. The energy level of the spin-singlet state was also determined in this study. The level is at $E_c - 0.20$ eV, where E_c denotes the minimum of the conduction band. Furthermore, a hydrogen-related center with tetrahedral symmetry in ion-implanted silicon was studied by means of infrared-absorption spectroscopy.[14] The center has been associated with the fully hydrogenated vacancy or with monosilane located at the interstitial tetrahedral site. All these experimental studies have provided us with examples supporting the assumption that the hydrogen atoms can sufficiently passivate silicon dangling bonds. Theoretical studies of the hydrogen-vacancy complexes in crystalline silicon have been performed.[15-17] However, detailed theoretical descriptions for the electronic structure of these complexes are not always available.

The purpose of this paper is to report on a systematic theoretical study for the electronic structure of the hydrogen-vacancy complexes in crystalline silicon using a self-consistent semiempirical tight-binding theory. The complex defects considered in this paper are those consisting of a vacancy and one through four hydrogen atoms being bonded to the nearest-neighbor silicon atoms of the vacancy. We model the defect systems by supercells, each containing 2662 lattice sites plus atomic sites of the hydrogen impurities and being subject to periodic boundary conditions. These supercells are large enough to eliminate rather completely the interdefect interactions. The defect electronic structure is calculated with the use of the recursion method (a real Green's-function method). By application of both the supercell and the recursion methods, we preserve the properties of the silicon

crystal well in the calculations, as would be achieved by using the standard Green's-function method, i.e., by solving for Dyson's equation. In addition, the combination of the two methods allows us to compute the defect states to a high accuracy and to avoid the finite-size effects which one would encounter in the calculations using a cluster method. It should be noted that only the electronic structure of the defect complexes is studied in this work. It is clear that the examination of total energies as functions of the positions of atoms is also very important. This is so in particular for the fully hydrogenated vacancy defect, i.e., the quadrihydrogen-vacancy complex, where the electronic activity of the vacancy is assumed to be completely passivated. However, we shall show in this work that the electrical activities should indeed remain in the other three considered hydrogen-vacancy complexes. Thus, one should be able to detect these defects by using electrical and optical techniques. Indeed, as we discussed before, both the DLTS (Ref. 13) and ODMR (Ref. 12) signals have been observed for the hydrogen-vacancy related complexes and have been assigned to the dihydrogen-vacancy defect. Therefore, our electronic-structure calculations are expected to be useful for experimentalists to confirm their assignments of the detected signals to the dihydrogen-vacancy defect and to identify the monohydrogen- and trihydrogen-vacancy complexes. In addition, we shall present the simple molecular-orbital models for the electronic structure of the four hydrogen-vacancy complexes, and we hope that such simple models are helpful in understanding the physical origin of the electronic properties of these complex defects.

The paper is organized as follows. In Sec. II a detailed description of the atomic configurations of the four complexes is presented. In Sec. III the theoretical approaches used in the calculations are described. The results of our calculations for the electronic structure of these four complex defects and the models which we propose for them are presented in Sec. IV. Comparison with available experiments and discussions are also given in this section. Section V contains a brief summary of the paper and conclusions.

II. CONFIGURATIONS OF HYDROGEN-VACANCY COMPLEXES

In the present work the four concerned hydrogen-vacancy complexes, namely, the mono-, di-, tri-, and quadri-hydrogen-vacancy complexes, in crystalline silicon, are denoted by VH, VH$_2$, VH$_3$, and VH$_4$, respectively. The atomic configurations in the central cell, defined as a vacancy plus its four first neighboring silicon atoms and the hydrogen atoms, are shown in Fig. 1. In VH$_4$, the four dangling bonds of the vacancy are all saturated by hydrogen atoms, while in the other three complexes, not all the dangling bonds are saturated. In the calculations, these four complexes are modeled by first removing a silicon atom from the crystal and then placing one through four hydrogen atoms at a distance of 0.90 Å from the vacancy center, without all other silicon atoms being displaced. These configurations give a silicon-hydrogen distance of 1.45 Å and a hydrogen-hydrogen distance of 1.47 Å, presenting a reasonable value of the silicon-hydrogen bond length since this bond length in the SiH$_4$ molecule is 1.48 Å. Further discussion about the choice of the value of 0.90 Å for the distance of the hydrogen atoms from the vacancy center will be presented later. In order to study the effect of symmetry-conserved distortions of the hydrogen atoms on the electronic structure, we also perform the calculations for the VH$_4$ defect with the hydrogen at distances of 0.65, 0.75, 1.05, and 1.20 Å from the vacancy center. When the Jahn-Teller distortion is considered, we will allow both hydrogen and silicon atoms to be displaced in order to see how the electronic structure of the defect is changed as the symmetry of the defect is lowered. However, for the sake of simplicity, the displacements will only be made for the atoms in the central cell of the defect.

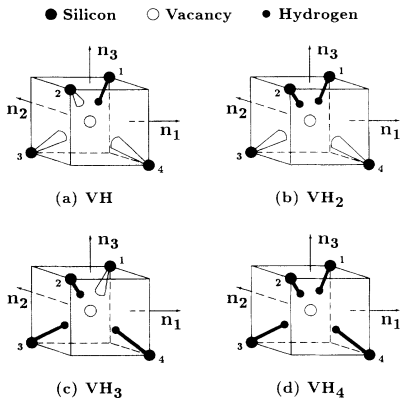

FIG. 1. Schematic illustration of the proposed atomic configuration for (a) the monohydrogen-vacancy (VH) complex in C_{3v} symmetry, (b) the dihydrogen-vacancy (VH$_2$) complex in C_{2v} symmetry, (c) the trihydrogen-vacancy (VH$_3$) complex in C_{3v} symmetry, and (d) the quadrihydrogen-vacancy (VH$_4$) complex in T_d symmetry in crystalline silicon. Only the central cells of the four complex defects are shown. The four silicon atoms in the central cell are labeled with integer numbers 1–4.

III. THEORETICAL METHOD

Our calculations are based on the self-consistent semiempirical tight-binding theory with the Wolfsberg-Helmholz formula[18] for the orbital interactions and the Sankey-Dow model of Coulomb effect[19] for the electron-electron interactions. The electronic structure of the perfect silicon crystal is described by an sp^3 first- and second-nearest-neighbor tight-binding Hamiltonian[20] and a large supercell.[21] The defect energy levels and the changes in the local densities of states induced by the defects are calculated using the Lanczos scheme[22] and the Haydock recursion method (a real-space Green's-function method),[23–25] respectively. The wave functions of the gap states are calculated with the use of a newly developed numerical method.[26] The hyperfine-interaction parameters arising from the paramagnetic spin of the electrons in the gap states of the complex defects alone are, in turn, derived from the calculated wave functions of the gap states.

A. Tight-binding Hamiltonian for the perfect crystal and description for the defect potential

In an sp^3 basis including both the first- and second-nearest-neighbor interactions, the Hamiltonian H_0 of the perfect crystal in the tight-binding approximation takes the form

$$H_0=\sum_{i,\sigma,\mathbf{R}}|i\sigma\mathbf{R}\rangle E_{0i}(\mathbf{R})\langle i\sigma\mathbf{R}| + \sum_{i,j,\sigma,\mathbf{R},\mathbf{R}'}|i\sigma\mathbf{R}\rangle V_{0ij}(\mathbf{R},\mathbf{R}')\langle j\sigma\mathbf{R}'| , \quad (1)$$

where $i=s$, p_x, p_y, or p_z labels the orbitals; σ is the spin ($\uparrow$ or $\downarrow$), and $\mathbf{R}$ denotes an atomic site vector. The transfer-matrix elements $V_{0ij}(\mathbf{R},\mathbf{R}')$ are taken as nonzero only between the nearest- and the second-nearest-neighbor atoms. The state $|i\sigma\mathbf{R}\rangle$ corresponds to a localized orbital centered on an atom at $\mathbf{L}$ or on an atom at $\mathbf{L}+\mathbf{d}$, where $\mathbf{L}$ is a lattice vector in the face-centered-cubic lattice and $\mathbf{d}=(1,1,1)a_0/4$ is the vector between nearest neighbors along the $\langle 111\rangle$ axis (a_0 is the cubic-lattice constant). In this work we use the tight-binding parametrization of the host energy band of the silicon crystal obtained by van der Rest and Pêcheur.[20] With this parametrization, success has been achieved in the study of the isolated vacancy,[27] vacancy pairs,[28,29] impurities,[20,30,31] and vacancy-impurity defect complexes[32] in silicon. The host crystal is further approximated by a large supercell[21] containing 2662 atoms and subject to periodic boundary conditions.

We can formally express the Hamiltonian of a defect as $H=H_0+U$, where U stands for the defect potential. In the sp^3 first- and second-nearest-neighbor tight-binding approach, the defect potential U can be written as

$$U=\sum_{i,\sigma,\mathbf{R}}|i\sigma\mathbf{R}\rangle U_i(\mathbf{R})\langle i\sigma\mathbf{R}| + \sum_{i,j,\sigma,\mathbf{R},\mathbf{R}'}|i\sigma\mathbf{R}\rangle U_{ij}(\mathbf{R},\mathbf{R}')\langle j\sigma\mathbf{R}'| . \quad (2)$$

In order to treat the defect potential for the complex defect containing the hydrogen impurities, we need to include hydrogen orbitals in our basis (see the Appendix for the general discussion on including the interstitial atomic orbitals in the basis of host crystal). However, only the hydrogen s orbitals are important and are included in our basis, because the energy of the p orbitals is much higher than that of the s orbitals. We keep all matrix elements, diagonal and off-diagonal, of the defect potential U for the vacant site, the hydrogen atoms, and the first- and second-nearest-neighbor silicon atoms, except for the off-diagonal elements between first- and second-nearest-neighbor silicon atoms. Here we note that since the recursion method is used in this work, the direct calculation of the matrix elements of the defect potential U is not a required step. This is in contrast to the standard Green's-function technique by which one has to solve the Dyson's equation and thus one has to know explicitly all the matrix elements of the defect potential U. Therefore, for convenience, we shall directly evaluate all the off-diagonal matrix elements of the Hamiltonian H for a defect.

For the vacant site, the diagonal matrix elements of the Hamiltonian H can be taken as infinite in magnitude and the off-diagonal matrix elements as zero. This standard procedure is just equivalent to decoupling the vacancy "atom" from the solid. For the first- and second-nearest-neighbor silicon atoms and for the hydrogen atoms, the off-diagonal matrix elements of the Hamiltonian H can be expressed in terms of the orbital interactions and are deduced from the corresponding off-diagonal matrix elements of the perfect crystal Hamiltonian H_0, while the diagonal matrix elements of H can be related to the electron occupations of orbitals and, therefore, need to be evaluated self-consistently. The determination of these Hamiltonian matrix elements will be described in Secs. III B and III C.

B. Orbital interactions

In our earlier studies of some other silicon vacancy-related complexes,[32] the off-diagonal Hamiltonian matrix elements corresponding to the orbital interactions between the first-nearest-neighboring atoms of the vacancy were calculated from the bulk values of the crystal with use of the Slater-Koster two-center approximation,[33] the Wolfsberg-Helmholz formula,[18] and the simplified Slater orbitals.[34–37] In this work we shall also use them to calculate the off-diagonal Hamiltonian matrix elements corresponding to the orbital interactions between the hydrogen and silicon atoms and between the hydrogen atoms themselves.

It was shown by Slater and Koster[33] that, in the two-center approximation, the off-diagonal Hamiltonian matrix element $V_{ll'}(\mathbf{R}_1,\mathbf{R}_2)$ corresponding to the interaction between orbital l centered on an atom at $\mathbf{R}_1$ and orbital l' centered on another atom at $\mathbf{R}_2$ can be expressed in terms of the two-center hopping integral $v_{ll'm}(R_{12})$, where $R_{12}=|\mathbf{R}_2-\mathbf{R}_1|$ stands for the distance between the two atoms, and $m=\sigma$ or π, as the conventional notation used in molecular-orbital theory refers to the component of angular momentum around the $(\mathbf{R}_2-\mathbf{R}_1)$ axis. We note that the two-center hopping integral is angle independent and the detail relation between $V_{ll'}(\mathbf{R}_1,\mathbf{R}_2)$ and $v_{ll'm}(R_{12})$ can be found in Ref. 33.

We shall further simplify our calculations by applying the Wolfsberg-Helmholz formula[18] to the two-center hopping integral $v_{ll'm}(R_{12})$. For the $v_{ll'm}(R_{12})$, the Wolfsberg-Helmholz formula reads

$$v_{ll'm}(R_{12})=\tfrac{1}{2}K_m(E_l+E_{l'})S_{ll'}(R_{12}) , \quad (3)$$

where E_l and $E_{l'}$ are the diagonal eigenvalues of the orbitals l and l', $S_{ll'}(R_{12})$ is the overlap integral between these two orbitals, and K_m is a constant. To calculate the overlap integral, we use the simplified Slater orbitals[34–37] of the type

$$R_l(r)=Ne^{-\mu_l r} , \quad (4)$$

where N is a normalization constant and μ_l is related to the eigenvalue E_l by

$$\hbar^2\mu_l^2/(2m)=-E_l . \quad (5)$$

The choice of the constant K_m in Eq. (3) is nevertheless rather difficult from fundamental or even empirical arguments. The way out of this problem is to express the matrix elements of H in terms of the corresponding bulk values of H_0, that is, to deduce the constants K_m from the matrix elements of H_0 using Eq. (3) and use them in the defect calculations. For further details of our approach to the off-diagonal matrix elements of the Hamiltonian H, see the Appendix and Refs. 35 and 36.

It is clear that the orbital interactions between a hydrogen atom and its bonding silicon atom play an essential role in passivation of the electrical activity of the silicon dangling bond. We believe that the behavior of these interactions is very similar to the behavior of the interactions in the perfect crystal between the first nearest neighbors and, therefore, these interactions are calculated from the bulk values of the first-nearest-neighbor interactions. The orbital interactions between hydrogen atoms themselves and between hydrogen atoms and silicon atoms with the nonhydrogenated dangling bonds should, however, behave differently from the bulk orbital interactions between the first nearest neighbors, because between these atoms there are no direct bondings. These orbital interactions should also behave differently from the bulk orbital interactions of the second nearest neighbors, because between these atoms there is a vacant region where an orbital orthogonality has been lifted. The above analyses guide us in this work to set the values of these orbital interactions to be at averages of the corresponding values calculated from the bulk values of the first-nearest-neighbor interactions and calculated from the bulk values of the second-nearest-neighbor interactions. The remaining orbital interactions involving hydrogen atoms should be weaker than the hydrogen-silicon orbital interactions we have just discussed. For the weaker hydrogen-silicon orbital interactions we will only include in the calculations those ones between a hydrogen atom and a silicon atom which is either chemically bonding to another hydrogen atom or a nearest neighbor of the silicon atom to which the hydrogen atom is bonded. These orbital interactions can be reasonably calculated from the bulk values of the second-nearest-neighbor interactions. Finally, the orbital interactions between the silicon atoms with dangling bonds are calculated from the bulk values of the first-nearest-neighbor interactions, exactly as we did in the calculations for the vacancy-related defects in silicon[32] and in III-V compound semiconductors.[36,37]

C. Self-consistency

For a hydrogen-vacancy complex defect, the rearrangement of the electronic charge will occur essentially in the region where the defect is located. To take into account effects of the charge rearrangement on the electronic structure of the defect, calculations should be self-consistent. In the present calculations, approximate self-consistency is obtained with the use of an empirical model of Coulomb effects developed by Sankey and Dow for impurities in semiconductors[19] and of a local charge-neutrality condition proposed by Xu and Lindefelt for an isolated vacancy in a semiconductor.[36,37]

In the latter case, taking as an example the neutral isolated silicon vacancy, the diagonal matrix elements E_s and E_p of the Hamiltonian H on the neighboring atoms of the vacancy are expressed as

$$E_s^1=E_{0s}+\Delta E^1 ,$$
$$E_p^1=E_{0p}+\Delta E^1 \tag{6}$$

and

$$E_s^2=E_{0s}+\Delta E^2 ,$$
$$E_p^2=E_{0p}+\Delta E^2 , \tag{7}$$

where E_{0s} and E_{0p} are the corresponding silicon bulk values and ΔE^1 and ΔE^2 are the energy shifts. We use superscripts 1 and 2 to indicate, respectively, the first and second nearest neighbors of the vacancy. With use of the local charge-neutrality condition,[36,37] ΔE^1 and ΔE^2 are adjusted such that the total charge on the four first-nearest-neighboring atoms of the vacancy is equal to the total charge on the four corresponding atoms in the perfect crystal and such that the total charge on the second-nearest-neighboring atoms is equal to the total charge on their corresponding atoms in the perfect crystal.

We first consider the $V\mathrm{H}_4$ defect, which can be handled by using the Sankey-Dow model[19] without invoking the charge-neutrality condition. In this model, atomic-orbital energies are expressed in terms of different electron repulsion parameters U_{ss}, U_{pp}, and U_{sp}, together with atomic bare ionization energies E_s^0 and E_p^0, as follows:

$$E_{s\sigma}(\{n_\alpha\})=E_s^0+\sum_{\sigma'}{}' n_{s\sigma'}U_{ss}+\sum_{j\sigma'} n_{p_j\sigma'}U_{sp} , \tag{8}$$

$$E_{p_i\sigma}(\{n_\alpha\})=E_p^0+\sum_{j\sigma'}{}' n_{p_j\sigma'}U_{pp}+\sum_{\sigma'} n_{s\sigma'}U_{sp} , \tag{9}$$

where i and $j=x$, y, or z; σ is the spin ($\uparrow$ or $\downarrow$); the prime on the summation indicates that the self-interaction is excluded; and n_α are the occupation numbers of spin orbitals $\alpha=i\sigma$. We adopt values for E_s^0, E_p^0, U_{ss}, U_{pp}, and U_{sp} as determined by Sankey and Dow,[19] who used the requirement that the Hartree-Fock s- and p-electron energies and the observed ionization potentials of free atoms should be reproduced. Using Eqs. (8) and (9), the atomic-orbital energies for the silicon atoms in the bulk crystal and for the hydrogen atoms and the first- and second-nearest-neighbor silicon atoms of the vacancy in the $V\mathrm{H}_4$ defect can easily be calculated. The diagonal matrix elements of the defect potential U are obtained by subtracting the calculated atomic-orbital energies for the silicon atoms in the bulk crystal from the calculated atomic-orbital energies for the hydrogen atoms and for the first- and second-nearest-neighbor silicon atoms of the vacancy. It is clear that the diagonal matrix elements of the Hamiltonian H are some functions of the orbital occupancies n_α, which in turn are fully determined by the Hamiltonian H. Therefore, the procedure of the calculations should be repeated iteratively until self-consistency is obtained.

Up to now, we have described the procedure for deter-

mination of the self-consistent defect potentials of the isolated vacancy and the $V\mathrm{H}_4$ defect in Si. For the $V\mathrm{H}$, $V\mathrm{H}_2$, and $V\mathrm{H}_3$ defects, we have both silicon-hydrogen bonds and silicon dangling bonds. To keep the calculations simple, we will only determine self-consistently the diagonal matrix elements of defect potential on the hydrogen atoms and on the four first-nearest-neighbor silicon atoms. The diagonal matrix elements of the defect potential on the second-nearest-neighbor silicon atoms of the vacancy are simply approximated by the values self-consistently determined for the isolated vacancy and the $V\mathrm{H}_4$ complex defect, in such a way that, for those which are first nearest neighbors of the silicon atoms with dangling bonds, the diagonal matrix elements are set equal to the values obtained for the isolated vacancy, while for those which are first nearest neighbors of the silicon atoms with silicon-hydrogen bonds, the diagonal matrix elements are set equal to the values obtained for the $V\mathrm{H}_4$ complex defect. We believe that this is a proper approximation, because the gap states are mainly derived from the silicon dangling orbitals and the major parts of the Coulomb effect are accounted for in the self-consistently calculated matrix elements of the defect potential on the hydrogen atoms and the first-nearest-neighbor silicon atoms.

In the calculations for the $V\mathrm{H}$, $V\mathrm{H}_2$, and $V\mathrm{H}_3$ defects, the atomic-orbital energies of the hydrogen atoms and the first-nearest-neighboring silicon atoms of the vacancy are all self-consistently determined using Eqs. (8) and (9). The corresponding matrix elements of the defect potential on all the hydrogen atoms and the silicon atoms which are directly bonded to the hydrogen atoms are then calculated by subtracting the calculated atomic-orbital energies for the silicon atoms in the bulk crystal from those for the hydrogen and silicon atoms in these defects. The corresponding matrix elements of the defect potential on the silicon atoms with dangling bonds are obtained by subtracting the calculated atomic-orbital energies of the silicon atoms for the isolated vacancy from those for these defects, plus the energy shift ΔE^1 determined for the isolated silicon vacancy by the local charge-neutrality condition described earlier in this paper. It is clear that the calculations need to be iterated until self-consistency is achieved.

D. The recursion method

The essential quantities in the present self-consistent calculations are the electronic spin-orbital occupancies n_α of the spin orbitals α. They can be obtained by integration of the corresponding local densities of states (LDOS) $\rho_\alpha(E)$,

$$n_\alpha = \int_{-\infty}^{E_F} \rho_\alpha(E) dE \ . \tag{10}$$

The local densities of states $\rho_\alpha(E)$ can in turn be expressed in terms of the Green's function $G(E) \equiv (E-H)^{-1}$ of a Hamiltonian H:

$$\rho_\alpha(E) = -\frac{1}{\pi} \lim_{\varepsilon \to 0} \mathrm{Im} G_\alpha(E+i\varepsilon) \ , \tag{11}$$

where $G_\alpha(E)$ stands for the diagonal matrix element of the Green's function corresponding to the spin orbital α. In the recursion method,[23,24] the diagonal matrix element $G_\alpha(E)$ is given by

$$G_\alpha(E) = \cfrac{1}{E-a_0-\cfrac{b_1^2}{E-a_1-\cfrac{b_2^2}{E-a_2-\cfrac{b_3^2}{E-\ddots}}}} \tag{12}$$

where a_n and b_n are recursion coefficients. They are generated, as we transform the Hamiltonian H to a tridiagonal form, by the recursion relation

$$b_{n+1}|u_{n+1}\rangle = H|u_n\rangle - a_n|u_n\rangle - b_n|u_{n-1}\rangle \ , \tag{13}$$

where $|u_n\rangle$ is a new orthonormal basis set starting with the first element $|u_0\rangle$ set equal to the spin orbital α. In principle, the continued fraction is infinite in length for an infinite solid, but in practice it always truncated at some finite level and the effects of the remaining tail of the continued fraction are approximated by a terminator $t(E)$. In this work, the square-root terminator[23,24] is used to generate the local densities of states $\rho_\alpha(E)$. This terminator replaces the band gap by a region with a low density of states.

It is clear that the above procedure can be used to calculate local densities of states for arbitrary linear combinations of the atomic orbitals in the basis. When the linear combinations are symmetrized according to the irreducible representations of the point symmetry group of a defect, the symmetric gap levels of the defect can be obtained by searching the poles in the diagonal matrix elements of the Green's function of the symmetrical combinations or the peaks in the corresponding local densities of states. The localizations of the defect levels can be estimated by integration of the corresponding changes of the local densities of states over the peaks.

This is a very efficient method for computing the integrated quantities through the energy bands and for identification of the resonances in the energy bands and the bound states in the gap. However, to locate the energy positions of the bound states and to calculate the level weights (projections) of the bound states on basis orbitals or their linear combinations, we have found it more convenient to use the Lanczos scheme[22] and the quadrature approach developed by Nex[25] for the recursion method.

When the recursion in Eq. (13) is truncated at a finite level N, an approximate tridiagonal Hamiltonian H^N of dimension $N+1$ is obtained:

$$H_N=\begin{bmatrix} a_0 & b_1 & 0 & 0 & 0 & 0 & & & \\ b_1 & a_1 & b_2 & 0 & 0 & 0 & & & \\ 0 & b_2 & a_2 & b_3 & 0 & 0 & & & \\ 0 & 0 & b_3 & a_3 & b_4 & 0 & & & \\ & & \ddots & \ddots & \ddots & & & & \\ & & & & & & a_{N-2} & b_{N-1} & 0 \\ & & & & & & b_{N-1} & a_{N-1} & b_N \\ & & & & & & 0 & b_N & a_N \end{bmatrix} . \tag{14}$$

In the Lanczos scheme,[22] the eigenvalues E_i^N and eigenvectors $|E_i^N\rangle$ of the Hamiltonian H^N are determined by solving directly the corresponding eigenvalue equation; the energy positions of the gap states are then obtained by searching the convergent eigenvalues in the gap as N increases.

The local densities of states and related quantities are alternatively calculated using the quadrature approach.[25] For the recursion truncated at level N, the local density of state $\rho_\alpha^N(E)$ is expressed in terms of the eigenvalues E_i^N and eigenvectors $|E_i^N\rangle$ of the H^N defined in Eq. (14):

$$\rho_\alpha^N(E)=\sum_{i=0}^{N}|\langle E_i^N|\alpha\rangle|^2\delta(E-E_i^N) = \sum_{i=0}^{N}\omega_{\alpha i}^N\delta(E-E_i^N) , \tag{15}$$

where $\omega_{\alpha i}^N$ is the weight (projection) of the eigenstate $|E_i^N\rangle$ on the orbital α. The corresponding electronic occupancy n_α^N is

$$n_\alpha^N=\int_{-\infty}^{E_F}\rho_\alpha^N(E)dE=\sum_{i}^{\text{occ}}\omega_{\alpha i}^N , \tag{16}$$

where the summation runs over occupied states only. The local density of state $\rho_\alpha(E)$ and electronic occupancy n_α of the orbital α are limit values of $\rho_\alpha^N(E)$ and n_α^N with $N\to\infty$:

$$\rho_\alpha(E)=\lim_{N\to\infty}\rho_\alpha^N(E) \tag{17}$$

and

$$n_\alpha=\lim_{N\to\infty}n_\alpha^N . \tag{18}$$

The central quantity for the calculation of the local density of states and the electronic occupancy in the quadrature approach is evidently the weight $\omega_{\alpha i}^N$. It has been shown by Nex[25] that the weight can be computed from the following equation:

$$\omega_{\alpha i}^N=\frac{q_N(E_i^N)}{p'_{N+1}(E_i^N)} , \tag{19}$$

where $p_N(E_i^N)$ and $q_N(E_i^N)$ are two polynomials satisfying the three-term recurrence relations

$$p_{n+1}(E_i^N)=(E_i^N-a_n)p_n(E_i^N)-b_n^2p_{n-1}(E_i^N) , \tag{20a}$$

$$q_{n+1}(E_i^N)=(E_i^N-a_{n+1})q_n(E_i^N)-b_{n+1}^2q_{n-1}(E_i^N) , \tag{20b}$$

with the initial conditions $p_{-1}(E_i^N)=q_{-1}(E_i^N)=0$, $p_0(E_i^N)=1$, and $q_0(E_i^N)=b_0^2=1$. The weight $\omega_{\alpha i}$ of the true eigenstates $|E_i\rangle$ is

$$\omega_{\alpha i}=\lim_{N\to\infty}\omega_{\alpha i}^N . \tag{21}$$

In all our calculations, we seldom need to go beyond $N=150$.

Again, the quadrature approach is applicable to computing local densities of states and related quantities for any linear combinations of the atomic orbitals in the basis. Using the Lanczos scheme and the quadrature approach, the energy positions and the projection weights of the bound states in the energy gap can easily be calculated to arbitrarily high accuracy.

E. Electronic wave functions of gap states

The wave functions of gap states of a defect are a kind of fundamental quantity that we need in order to compute the hyperfine fields of the defect (see Sec. III F). Once the energy positions of these gap states and their projection weights on the basis functions are accurately determined, their electronic wave functions can easily be calculated using a numerical method introduced recently by Xu.[26] Here, we give only a brief outline of the method. More details can be found elsewhere.[26]

The wave function $|\psi\rangle$ of a gap state with eigenenergy E can be expressed as a linear combination of the basis orbitals ($|\phi_\alpha\rangle$, $\alpha=i\mathbf{R}$, $i=s, p_x, p_y$, or p_z) as follows:

$$|\psi\rangle=\sum_\alpha e^{i\theta_\alpha}(\omega_\alpha)^{1/2}|\phi_\alpha\rangle , \tag{22}$$

where ω_α, which is always positive, is the projection weight of the gap state on the basis orbital $|\phi_\alpha\rangle$ and $e^{i\theta_\alpha}$ is the phase factor. The phase shift $\theta_\alpha=0$ or π needs to be determined. We note that we have dropped the spin label in both sides of Eq. (22) and the summation over $\mathbf{R}$ should be understood to run through both hydrogen and silicon atomic sites [cf. Eqs. (1) and (2)]. The projection weights $\{\omega_\alpha\}$ satisfy the normalization condition

$$\sum_\alpha\omega_\alpha=1 . \tag{23}$$

Since only relative phase shifts have an effect on the physical results, we can choose, without losing any generality, any one of the phase shifts to be zero. To keep the notation even simpler, we let the α take positive in-

teger numbers and the phase shift θ_1 be zero, assuming $\omega_1 \neq 0$. The wave function $|\psi\rangle$ can then be written as

$$|\psi\rangle = (\omega_1)^{1/2}|\phi_1\rangle + \sum_{\alpha=2} e^{i\theta_\alpha}(\omega_\alpha)^{1/2}|\phi_\alpha\rangle \ . \tag{24}$$

In order to determine the values for the phase shifts, we define a test orbital for each α ($\alpha \neq 1$):

$$|\tilde{\varphi}_\alpha(\tilde{\theta}_\alpha)\rangle = \frac{1}{(\omega_1+\omega_\alpha)^{1/2}}[(\omega_1)^{1/2}|\phi_1\rangle + e^{i\tilde{\theta}_\alpha}(\omega_\alpha)^{1/2}|\phi_\alpha\rangle] \ , \tag{25}$$

with a trial phase shift $\tilde{\theta}_\alpha$. The projection weight of the gap state on the test orbital is

$$\tilde{\omega}_\alpha(\tilde{\theta}_\alpha) \equiv |\langle\tilde{\varphi}_\alpha(\tilde{\theta}_\alpha)|\psi\rangle|^2 = \left|\frac{\omega_1+\omega_\alpha \exp[i(\theta_\alpha-\tilde{\theta}_\alpha)]}{(\omega_1+\omega_\alpha)^{1/2}}\right|^2 . \tag{26}$$

Here, we have used the orthonormality property of the basis orbitals. We obviously have

$$\tilde{\omega}_\alpha = \begin{cases} \omega_1+\omega_\alpha & \text{if } \tilde{\theta}_\alpha-\theta_\alpha=0 \\ |\omega_1-\omega_\alpha|^2/(\omega_1+\omega_\alpha) & \text{if } \tilde{\theta}_\alpha-\theta_\alpha=\pi \end{cases} \tag{27}$$

and

$$|\omega_1-\omega_\alpha|^2/(\omega_1+\omega_\alpha) \leq \tilde{\omega}_\alpha(\tilde{\theta}_\alpha) \leq \omega_1+\omega_\alpha \ . \tag{28}$$

This suggests a numerical procedure for the determination of the phase shifts $\{\theta_\alpha\}$ in Eq. (24) as follows. We first construct a test function for each α using Eq. (25) and calculate the projection weights of the gap state on the test orbital with the trial phase shift $\tilde{\theta}_\alpha=0$ and $\tilde{\theta}_\alpha=\pi$ using Eq. (19). The correct values of the phase shifts $\{\theta_\alpha\}$ in the expansion of the wave function of the gap state [Eq. (24)] are determined by the following rule: If $\tilde{\omega}_\alpha(\tilde{\theta}_\alpha=0)=\omega_1+\omega_\alpha$, then $\theta_\alpha=0$, whereas if $\tilde{\omega}_\alpha(\tilde{\theta}_\alpha=\pi)=\omega_1+\omega_\alpha$, then $\theta_\alpha=\pi$. Once all values of the phase shifts $\{\theta_\alpha\}$ are determined, the wave function of the gap state follows simply by inserting them into Eq. (24).

We make the following notes about the method. First, the method does not require any information about the eigensolutions other than the gap state of one's interest to be used as inputs. Secondly, when the gap state is very localized, its wave function can be expanded in a small number of the basis orbitals and, correspondingly, our numerical procedure need only run for very few phase shifts. Even further, the signals detected by many experimental techniques only correlate to the partial wave functions of gap states. The computation of the partial wave functions is then a key step in the theoretical interpretation of the corresponding experimental results and can be done very quickly using our method. Finally, for a defect system with some symmetry properties, one can reduce the number of the phase shifts which need to be numerically determined if the orbitals in the basis are symmetrized.

F. Hyperfine interaction

Experimental techniques such as electron paramagnetic resonance (EPR) probe the interaction between electronic wave functions and nuclear spins. When applied to a defect in a semiconductor, the spectra of such techniques, properly interpreted, contain highly detailed microscopic information about the structure of the defect which often cannot be obtained in any other way. However, the conclusive structural identification of the defect may only be obtained if theoretical calculations of the hyperfine-interaction parameters for various configurations are available.

The hyperfine-interaction parameters are often presented as a tensor which is known as the hyperfine-interaction tensor. For a defect in a semiconductor, the elements of the tensor can be analyzed in terms of three different contributions.[38] The first contribution arises from the paramagnetic spin of the electronic wave function of the gap state. This contribution actuates the electron hyperfine field of the defect. As a consequence of the wave function of the gap state, one will have a contribution to the elements of the hyperfine-interaction tensor from a spin polarization of the valence band, and also a contribution from a spin polarization of the atomic core states. In this paper we shall disregard the contributions to the hyperfine-interaction tensor from the two types of spin polarizations. This is a crucial approximation. In a recent calculation for chalcogen point defects and defect pairs in silicon,[38] Overhof, Scheffler, and Weinert showed that the contributions from the spin polarizations, particularly of the valence band to the hyperfine-interaction tensor elements, can be quite significant. However, at the chalcogen nuclei the contributions from the spin polarizations were found to be relatively unimportant. At the nearest-neighbor silicon nuclei of the chalcogen impurities, except for Te impurity, the major contributions to the hyperfine-interaction tensor elements are found to still come from the wave function of the gap state. In this work we will only consider the hyperfine-interaction tensor for the hydrogen nuclei and the silicon nuclei at the nearest-neighbor sites of the vacancy. Therefore, although only the hyperfine-interaction tensor elements deduced from the paramagnetic spin of the electronic wave function of the gap state are presented, we expect that our results can still be useful in analyses of EPR and ODMR experiments.

The direction of the principal axis of the hyperfine-interaction tensor is also of importance in the microscopic identification of defects. Since the electron hyperfine field is actuated by the paramagnetic spin of the electronic wave function of the gap state, it should be well to assign the direction of the symmetric axis of the partial wave function of the gap state at each atomic site to the direction of the principal axis of the hyperfine-interaction tensor at the corresponding nucleus (see also discussions below).

The hyperfine interactions arising only from magnetic interactions between nuclei and paramagnetic spin of the electronic wave function of the gap state are described by the Hamiltonian given by[39]

$$H_{hf}=\sum_{\mathbf{R}}\mathbf{S}\cdot\overleftrightarrow{A}(\mathbf{R})\cdot\mathbf{I}(\mathbf{R}) , \tag{29}$$

where the sum goes over all atomic sites $\mathbf{R}$, $\mathbf{I}(\mathbf{R})$ is the nuclear spin, $\mathbf{S}$ the total spin vector of the unpaired electrons in the gap state, and $\overleftrightarrow{A}(\mathbf{R})$ is the hyperfine interaction tensor and can be calculated by[39]

$$A_{ij}=g_e g_n \mu_B \mu_n \left[\frac{8\pi}{3}|\psi(0)|^2\delta_{ij}+\left\langle\frac{3r_i r_j}{r^5}-\delta_{ij}\frac{1}{r^3}\right\rangle\right] , \tag{30}$$

where r_i and r_j are the components of the position vector $\mathbf{r}$ from the nucleus at $\mathbf{R}$ to the electrons with the spin $\mathbf{S}$. g_e is the electron g value and g_n is that of the nucleus. μ_B is the Bohr magneton and μ_n the nuclear magneton. The term with $|\psi(0)|^2$, the electron probability density at the nucleus, is the Fermi contact term, which is isotropic. The second term in Eq. (30) is the dipole-dipole interaction term, which is anisotropic. The angular brackets in this term mean an average taken over the wave functions of the unpaired electrons in the gap state.

In order to make our theoretical results easier to compare with experiments, we rewrite the wave functions of the gap states [Eq. (22)] as follows:

$$|\psi\rangle=\sum_{\mathbf{R}}\eta(\mathbf{R})|\Phi(\mathbf{R})\rangle , \tag{31}$$

where $|\eta(\mathbf{R})|^2$ is the projection weight of the wave function of the gap state on the atomic orbital $|\Phi(\mathbf{R})\rangle$ centered at site $\mathbf{R}$. The atomic orbital $|\Phi(\mathbf{R})\rangle$ is further defined as a linear combination of an s- and a p-like orbital as follows:

$$|\Phi(\mathbf{R})\rangle=\alpha(\mathbf{R})|\phi_s(\mathbf{R})\rangle+\beta(\mathbf{R})|\phi_p(\mathbf{R})\rangle , \tag{32}$$

where $|\alpha(\mathbf{R})|^2+|\beta(\mathbf{R})|^2=1$. Comparing Eqs. (31) and (32) with Eq. (22), we obtain the relations between the coefficients $\eta(\mathbf{R})$, $\alpha(\mathbf{R})$, and $\beta(\mathbf{R})$ and the coefficients $e^{i\theta_\alpha}(\omega_\alpha)^{1/2}$ ($\alpha=i\mathbf{R}$, $i=s, p_x, p_y$, and p_z):

$$\begin{aligned}
&|\eta(\mathbf{R})|^2=\omega_{s\mathbf{R}}+\omega_{p_x\mathbf{R}}+\omega_{p_y\mathbf{R}}+\omega_{p_z\mathbf{R}} ,\\
&|\alpha(\mathbf{R})|^2=\omega_{s\mathbf{R}}/|\eta(\mathbf{R})|^2 ,\\
&|\beta(\mathbf{R})|^2=(\omega_{p_x\mathbf{R}}+\omega_{p_y\mathbf{R}}+\omega_{p_z\mathbf{R}})/|\eta(\mathbf{R})|^2 .
\end{aligned} \tag{33}$$

The direction of the lobe of the p-like function in Eq. (32) is defined by three direction cosines l, m, and n,

$$\begin{aligned}
&l=e^{i\theta_{p_x}}(\omega_{p_x})^{1/2}/|\beta| ,\\
&m=e^{i\theta_{p_y}}(\omega_{p_y})^{1/2}/|\beta| ,\\
&n=e^{i\theta_{p_z}}(\omega_{p_z})^{1/2}/|\beta| .
\end{aligned} \tag{34}$$

Here the suffix $\mathbf{R}$ has been dropped.

It is a commonly adopted assumption[40,41] that only the atomic orbitals centered on the atomic site $\mathbf{R}$ have contributions to $\overleftrightarrow{A}(\mathbf{R})$ and the contributions from the other atomic orbitals are neglected. Under this assumption, it can be seen from Eq. (30) that the hyperfine-interaction tensor $\overleftrightarrow{A}$, arising from the wave function of the gap state alone, is axially symmetric around the axis along the direction of the lobe of the p-like function centered on the atomic site $\mathbf{R}$. Thus, the tensor $\overleftrightarrow{A}(\mathbf{R})$ from the nucleus at site $\mathbf{R}$ can, in general, be described as[40,41]

$$A_{\parallel}(\mathbf{R})=a(\mathbf{R})+2b(\mathbf{R}) , \tag{35a}$$

$$A_{\perp}(\mathbf{R})=a(\mathbf{R})-b(\mathbf{R}) , \tag{35b}$$

where the hyperfine parameters a and b are given by

$$a=\frac{8\pi}{3}g_e g_n \mu_B \mu_n |\alpha|^2 |\eta|^2 |\psi_s(0)|^2 \tag{36a}$$

and

$$b=\tfrac{2}{5}g_e g_n \mu_B \mu_n |\beta|^2 |\eta|^2 \langle r^{-3}\rangle_p . \tag{36b}$$

The suffix $\mathbf{R}$ has again been dropped in these two equations. $|\psi_s(0)|^2$ in Eq. (36a) is the amplitude of the s-like atomic orbital at the nucleus at site $\mathbf{R}$, and $\langle r^{-3}\rangle_p$ in Eq. (36b) is the expectation value of r^{-3} weighted over the p-like atomic orbital centered on the site $\mathbf{R}$. In this work we shall not attempt to calculate the values of $|\psi_s(0)|^2$ and $\langle r^{-3}\rangle_p$ for the atoms in question. Instead, we shall use the values derived from the Hartree-Fock-Slater atomic orbitals,

$$|\psi_s(0)|^2=34.52\times10^{24}\ \text{cm}^{-3}$$

and

$$\langle r^{-3}\rangle_p=18.16\times10^{24}\ \text{cm}^{-3} ,$$

for the silicon atoms,[42] and the value derived from the free atomic $1s$ orbital,

$$|\psi_s(0)|^2=2.148\times10^{24}\ \text{cm}^{-3} ,$$

for the hydrogen atoms.[43] These values were used in Ref. 12 where the VH_2 defect in silicon was studied by the ODMR technique.

IV. RESULTS AND DISCUSSION

In this section the results of our calculations will be presented and analyzed. In order to have a better understanding of the physical origin of the calculated electronic structures, a set of qualitative models in terms of one-electron molecular orbitals will be constructed for the considered hydrogen-vacancy complexes. We shall also make comparison of the results of our calculations with experimental studies.

At the outset, we define the orbitals on which the LDOS's we discussed throughout this section are projected. Even our self-consistent potential for a defect considered in this paper has been determined approximately for the hydrogen atoms and the first- and second-nearest-neighbor silicon atoms of the vacancy in the defect; we shall only discuss our calculated LDOS's for the orbitals centered on the atoms shown in Fig. 1, that is, in the central cell of the defect. At times, we will also discuss the calculated results for the isolated silicon vacancy. In this case, the orbitals on which the considered LDOS's are projected are simply those centered on the

four nearest-neighbor silicon atoms of the vacancy (the central cell of the vacancy). Our calculated change in the LDOS (ΔLDOS) presented in this section is defined as the difference between the sum of the LDOS's corresponding to all the orbitals centered on the atoms in the central cell of the defect and the sum of the LDOS's calculated for the perfect crystal corresponding to all the orbitals centered on a silicon atom and its four nearest-neighbor atoms in the crystal. In order to obtain the symmetrical properties of defect states, all the considered orbitals have been symmetrized according to the irreducible representations in the point symmetry group of the defect.

A. Quadrihydrogen-vacancy (VH_4) complex

We begin by first presenting our results for the VH_4 defect, because this defect is the most studied of the hydrogen-vacancy complexes and because its electronic structure can be very easily understood. In Fig. 2 we show the calculated ΔLDOS's of different symmetries for the atoms in the central cell of the defect. The results presented in this figure are obtained for a configuration in which the hydrogen atoms have been placed a distance of 0.90 Å from the vacancy center. It is clear that there are no significant changes in the LDOS of the e and t_1 symmetries. In Fig. 2 we have not shown ΔLDOS for the a_2 symmetry, because with an sp^3 basis, the a_2 linear combination cannot be obtained from the orbitals centered on the atoms in the central cell of the defect. We can, however, expect an even smaller change in the density of states for this symmetry. Figure 2 shows that the VH_4 defect induces two sharp peaks in the ΔLDOS of a_1 symmetry and a sharp and a broadened peak in the ΔLDOS of t_2 symmetry. There is no electrically active state in the fundamental band gap.

As discussed earlier, it is a reasonable first guess to place the hydrogen atoms at a distance $d=0.90$ Å from the vacancy center. To judge this guess, we calculate the electronic structure of the defect with the hydrogen atoms at other distances d from the vacancy center. The silicon atoms are always kept at the same positions. Figure 3 shows the results of our calculations for $d=0.65$, 0.75, 1.05, and 1.20 Å, together with the results for $d=0.90$ Å and the results for the undistorted isolated silicon vacancy for comparison. In this figure only the results for the ΔLDOS's of a_1 and t_2 symmetries are shown. The ΔLDOS's of the e and t_1 symmetries remain very small. It is found that the global electronic structure of the defect is same for these different d values. However, quantitative differences in the calculated results for the different d values occur. For $d=0.65$ and 0.75 Å, the upper a_1 state of the VH_4 defect stays in the fundamental band gap, while the lower t_2 state interacts with the valence states of the crystal, forming a very broad resonance state and giving a good recovery of the electronic structure of the crystal valence band of t_2 symmetry. As d is increased, the position of the upper a_1 state shifts towards higher energy and eventually into the conduction band, while the position of the lower t_2 state in the valence band shifts towards lower energy and the

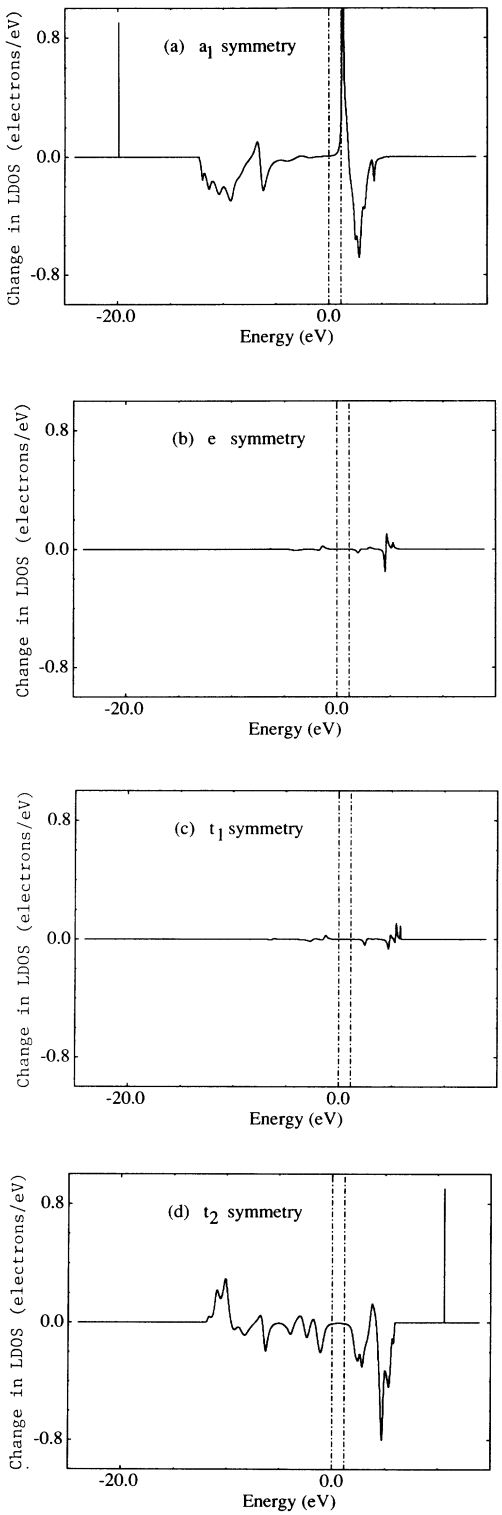

FIG. 2. Calculated changes in the local densities of states (ΔLDOS) of (a) a_1, (b) e, (c) t_1, and (d) t_2 symmetries induced by the neutral VH_4 defect (in T_d symmetry) in crystalline silicon with the hydrogen atoms being placed a distance of $d=0.90$ Å from the vacancy center, corresponding to all the atomic sites in the central cell of the defect. Units are electrons per eV. The spin degeneracy is excluded. The energy at the top of the valence band is set to zero. The edges of the fundamental band gap are identified by dot-dashed lines.

localization of the state is increased, which indicates that the recovery of the valence electronic structure is getting worse. On balance, the choice of $d=0.90$ Å seems reasonable. In addition, these results show that when the hydrogen atoms are moved away from their bonding silicon atoms, an empty a_1 gap state drops out from the conduction band.

By comparison of these results with the calculated ΔLDOS's for the undistorted isolated silicon vacancy, we immediately see that the a_1 resonance state of the silicon vacancy is pushed out from the valence band, while the t_2 bound state is pushed away from the fundamental band gap. This electronic structure of the defect can be well described by a model presented in Fig. 4. In the model, the four hydrogen s orbitals are symmetrized, giving an a_1 and three degenerate t_2 combinations [Fig. 4(a)]. The same symmetrizations are done for the four hybrid orbitals on the nearest-neighbor silicon atoms of the vacancy, pointing towards the vacancy center [Fig. 4(c)]. In order to have the relative energy positions of the symmetrized orbitals right, we have calculated the projection weights of the lower a_1 and the upper t_2 state on the atoms in the central cell of the defect for $d=0.90$ Å, even though these two states may have no physical relevance for the electronic and optical properties of the defect. We have found that 81% (18%) of the wave function of the lower a_1 state well below the valence band is localized on the four hydrogen (silicon) atoms in the central cell of the defect, while 67% (30%) of the wave function of the upper t_2 state well above the lowest conduction band is local-

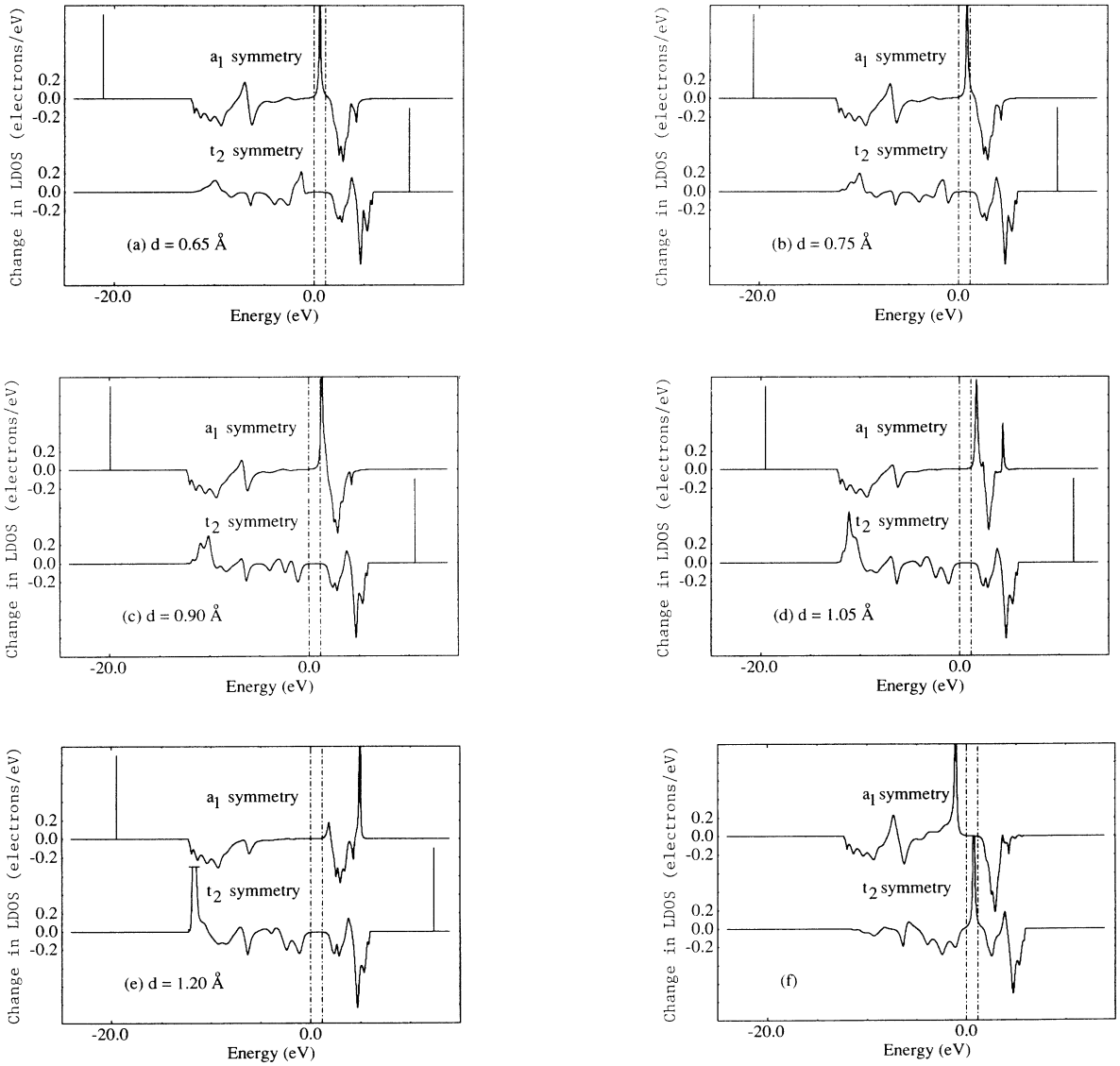

FIG. 3. Calculated changes in the local densities of states (ΔLDOS) of a_1 and e symmetries induced by the neutral VH_4 defect in crystalline silicon, for all the atomic sites in the central cell of the defect for the hydrogen atoms at a distance of (a) $d=0.65$ Å, (b) $d=0.75$ Å, (c) $d=0.90$ Å, (d) $d=1.05$ Å, and (e) $d=1.20$ Å from the vacancy center. (f) is the calculated corresponding ΔLDOS for the undistorted isolated silicon vacancy. Units are electrons per eV. The spin degeneracy is excluded. The energy at the top of the valence band is set to zero. The edges of the fundamental band gap are identified by dot-dashed lines.

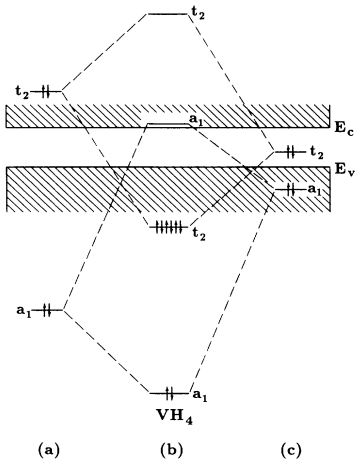

FIG. 4. Schematic illustration of the one-electron molecular-orbital treatment for the electronic structure of the neutral $V\mathrm{H}_4$ defect (in T_d symmetry) in crystalline silicon. (a) shows an a_1 and a t_2 level associated with the linear combinations of the four hydrogen s orbitals. (c) shows an a_1 and a t_2 level formed from the four silicon hybrids surrounding the vacancy. (b) is the energy-level scheme of the $V\mathrm{H}_4$ defect resulting from the interactions between the two a_1 levels and between the two t_2 levels shown in (a) and (c). The four Si-H bonds are formed as the a_1 and t_2 bonding states are fully occupied by eight electrons.

ized on the four hydrogen (silicon) atoms. These results lead us to place the a_1 (t_2) combination of the hydrogen orbitals below (above) the a_1 (t_2) combination of the silicon hybrid orbitals. The defect states of $V\mathrm{H}_4$ are finally formed by the interactions between the symmetrized hydrogen s and silicon hybrid orbitals, giving a bonding and an antibonding a_1 state and a bonding and an antibonding t_2 state [Fig. 4(b)]. Due to the interactions, the t_2 gap level of the isolated silicon vacancy has been removed from the fundamental band gap. The four Si-H bonds in the defect are formed as the a_1 and t_2 bonding states are fully occupied by electrons. This feature of passivation of the silicon dangling bonds is different from that by the substitutional group-V impurity atoms in the quadrigroup-V–vacancy complexes,[32] where the deactivation of the electrical properties of the isolated silicon vacancy is due to the lowering of the energies of the dangling orbitals by the group-V impurity ions.

Our results are, in general, consistent with other similar calculations,[15–17] even though different theoretical approaches have been used. However, no detailed comparisons between those calculations and ours will be made in this paper.

B. Monohydrogen-vacancy ($V\mathrm{H}$) complex

In the ($V\mathrm{H}$) defect, the hydrogen atom can saturate one of the silicon dangling bonds pointing towards the vacancy center. In the absence of Jahn-Teller distortions, a typical configuration of the defect is illustrated in Fig. 1(a), where only the central cell of the defect is shown and the hydrogen atom is placed a distance of 0.90 Å from the vacancy center or, equivalently, 1.45 Å from its bonding silicon atom (Si_1). The point symmetry group of the defect in this case is C_{3v}. We have done calculations for the neutral defect in this symmetry. Figure 5 shows the calculated ΔLDOS's of the a_1 and e symmetries for all atomic sites in the central cell of the defect. It can be seen that for the a_1 symmetry, the $V\mathrm{H}$ defect has a strong resonance at an energy just below the upper edge of the valence band and a defect state at an energy above the lowest conduction band. For the e symmetry, the defect introduces a bound state in the fundamental band gap. In Table I the energy positions of these defect states have been listed. We note that for the defect in its neutral state, the e symmetry gap state is at $E_v+0.72$ eV (E_v denotes the upper edge of the valence band), the same energy position as the t_2 gap state of the ideal isolated silicon vacancy.[32] In Fig. 5, we have not shown the calculated ΔLDOS of a_2 symmetry. We here note that, as for the LDOS's of e and t_1 symmetries of the $V\mathrm{H}_4$ defect, we have found that the $V\mathrm{H}$ defect does not introduce any significant change in the LDOS of a_2 symmetry.

In the central cell of the $V\mathrm{H}$ defect, the atoms can be divided into three groups such that in each group the atoms are symmetrically equivalent. The three groups are the following: one consisting of only the hydrogen atom, one only the Si_1 atom, and one the other three silicon atoms (Si_2, Si_3, and Si_4). We have done the calculations for the localizations of the a_1 and e defect states on each of the three groups of atoms. The results are also listed in Table I. It is shown that the a_1 resonance state in the valence band and the e gap state at $E_v+0.72$ eV appear mainly as the combination of the atomic orbitals of the three silicon atoms (atoms Si_2, Si_3, and Si_4) which have not been saturated by the hydrogen atom, whereas the a_1 state at an energy above the lowest conduction band appears essentially as a combination of the orbitals of the hydrogen atom and its bonding silicon atom Si_1. We note that the calculated results for the a_1 state located above the lowest conduction band may still have no physical relevance for the electronic and optical proper-

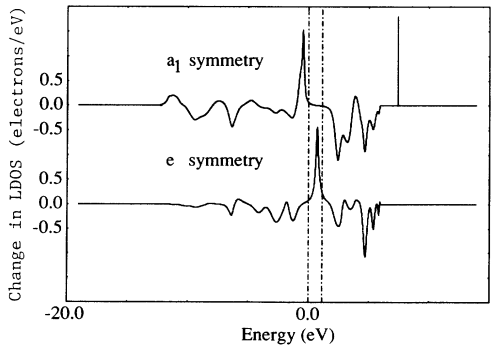

FIG. 5. Calculated changes in the local densities of states (ΔLDOS) of a_1 and e symmetries induced by the neutral $V\mathrm{H}$ defect (in C_{3v} symmetry) in crystalline silicon, corresponding to all the atomic sites in the central cell of the defect. Units are electrons per eV. The spin degeneracy is excluded. The energy at the top of the valence band is set to zero. The edges of the fundamental band gap are identified by dot-dashed lines.

TABLE I. Calculated a_1 and e energy levels in and around the fundamental band gap and their localization characters α_j, β_j, and η_j for the neutral and non-Jahn-Teller-distorted VH defect in silicon. The energies of the levels are measured relative to the top of the valence band. The point symmetry group of the defect is C_{3v}. The sum over j in column 7 runs over the equivalent atoms only. The level localization is defined as the sum of the localizations of a defect state on all atoms in the central cell of the defect. The column labeled level occupancy indicates electron occupation of the levels of the neutral defect.

Energy level (eV)	Symmetry	Atomic identity	Number of equivalent atoms	α_j^2	β_j^2	$\sum_j \eta_j^2$	Level localization	Level occupancy
−0.41	a_1	H	1	1.00		0.011	0.70	2
		Si_1	1	0.10	0.90	0.032		
		Si_2	3	0.11	0.89	0.652		
0.72	e	Si_1	1		1.00	0.000	0.64	1
		Si_2	3	0.20	0.80	0.643		

ties of the defect, but again they can be used as a clue to the physical origin of the defect states in and around the fundamental band gap.

In Fig. 6 we show the model that we propose to explain our computational results. The s orbital of the hydrogen atom interacts strongly with the Si_1 hybrid orbital pointing towards the hydrogen atom, giving a bonding and an antibonding a_1 state with a large energy separation [Fig. 6(a)]. The formation of the Si-H bond is due to the occupation of two electrons on the a_1 bonding state. This Si-H bond resembles very well the Si-Si bond of the silicon crystal in the electronic properties and, thus, gives contributions to the valence band in a wide range of energies. Therefore, no localized defect state mainly associated with the a_1 bonding state has been found in the valence band (see Fig. 5 and Table I). The three silicon dangling bonds pointing to the vacancy center are symmetrically equivalent and can thus be symmetrized according to the irreducible representations of the point symmetry group C_{3v}, giving an a_1 and an e symmetry state [Fig. 6(d)]. It is clear that the e gap state of the VH defect stems from the e symmetry state of the three silicon dangling bonds and, therefore, stays at the same energy position as the t_2 gap state of the isolated silicon vacancy. However, a weak interaction between the a_1 state of the three silicon dangling bonds and the Si-H antibonding state is expected to occur and, thus, a very small contribution to the a_1 resonance state of the VH defect from the hydrogen and Si atoms is found (see Table I). All these discussions are summarized in Fig. 6(c).

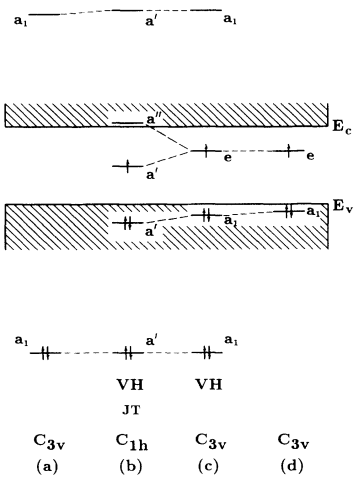

FIG. 6. Schematic illustration of the one-electron molecular-orbital treatment for the electronic structure of the neutral VH defect in crystalline silicon. (a) shows two a_1 energy levels associated with a bonding and an antibonding combination of the hydrogen s orbital and the hydrogen-saturated silicon hybrid towards the vacancy center. (d) shows an a_1 and an e energy level formed from the three silicon dangling orbitals. (c) is the energy-level scheme of the VH defect in C_{3v} symmetry, obtained simply by the combination of the results shown in (a) and (d). A very weak interaction between the a_1 antibonding combination of the hydrogen s orbital and the hydrogen-saturated silicon hybrid and the a_1 combination of the silicon dangling bonds is indicated in (c). (b) shows the electronic structure for the defect after a Jahn-Teller (JT) distortion, which lowers the defect symmetry from C_{3v} to C_{1h}. The Si-H bond is formed as two electrons are accommodated in the bonding state formed from the hydrogen s orbital and the hydrogen-saturated silicon hybrid.

Clearly, the VH defect in its neutral state should undergo a Jahn-Teller distortion, since the fourfold-degenerate (including spin) e level is occupied by only one electron. A possible Jahn-Teller distortion is that two silicon atoms (for example, the Si_3 and Si_4 atoms) with dangling bonds pull together to form a pair-bonding state and the remaining one (the Si_2 atom) moves away from the vacancy center. The Jahn-Teller distortion will lower the symmetry of the defect from C_{3v} to C_{1h} and, thus, cause a splitting of the e level according to $e=a'+a''$ with the spin-unpaired electron at the a' gap state. A schematic description for the electronic structure of the Jahn-Teller-distorted VH complex defect is shown in Fig. 6(b).

The VH defect in its neutral state is clearly an electron paramagnetic resonance active center. Table II gives the calculated hyperfine-interaction parameters and coefficients of the spin-unpaired electron wave function for the atoms in the central cell of the defect after two assumed Jahn-Teller distortions. In each case, only the three silicon atoms (Si_2, Si_3, and Si_4) with dangling bonds and the hydrogen atom have been distorted, while the

hydrogen-saturated Si_1 atom has been fixed on its C_{3v} symmetric position shown in Fig. 1(a). In the first (second) case, the x and y coordinates of the hydrogen atom and the Si_2, Si_3, and Si_4 atoms have been displaced by 10% (20%) from their C_{3v} symmetric positions of Fig. 1(a) and the z coordinate of the hydrogen atom by 20% (40%). In Table II, in addition to its three direction cosines l, m, and n, the axial direction of the hyperfine tensor for an atom (Si_1 or Si_2) in the mirror plane of the defect is also presented by the angle θ ($0° \leq \theta \leq 180°$) between the axial direction and the $\langle 110 \rangle$ direction in the mirror plane. It can be seen that 50% of the spin-unpaired electron wave function is localized on the Si_2 atom, and 10% on the Si_3 and Si_4 atoms. Contributions to the unpaired electron wave function from the hydrogen and Si_1 atoms are negligibly small. The axial direction of the hyperfine tensor at the atomic site Si_2 is found to be almost parallel to the $\langle \bar{1}\bar{1}1 \rangle$ direction or to the dangling-bond direction of the Si_2 atom in the isolated ideal vacancy. The axial directions of the hyperfine tensors at the atomic sites Si_3 and Si_4 have been slightly oriented towards to the directions favorable to form a pair bonding between the two atoms. These results are found to have a very small dependence on the magnitude of the Jahn-Teller distortion, as can be seen by comparison of the calculated results for the two assumed Jahn-Teller distortions (Table II). However, the spin-unpaired electron energy level is indeed lowered by the Jahn-Teller distortion. This lowering can exceed the increase in energy of the level caused by condensing the unpaired electron state to only one silicon dangling orbital (see case II of Table II). The axial direction of the hyperfine tensor at the atomic site Si_1 is also changed with the Jahn-Teller distortion in a trend towards the $\langle 111 \rangle$ direction (i.e., towards $\theta = 35.26°$). This is in accord with that when the Jahn-Teller distortion is nearly vanishing; the axial direction of the hyperfine tensor should be nearly perpendicular to the $\langle 111 \rangle$ direction.

There are no experimental results on the VH defect with which our calculated results can be compared. However, it has been found that the unpaired electron states in the VH defect and in the VP defect, i.e., the silicon E center,[41] are very similar in many aspects, such as the localizations of the unpaired electron states and the hyperfine tensors at silicon atomic sites surrounding the vacancy. This could result in a difficulty in distinguishing the experimental signals of the VH defect from that of the VP defect. A clue to identification of the VH defect is, of course, the Si-H bond which should give contributions to the infrared-absorption spectra. In addition, a small but not vanishing localization of the unpaired electron state on the hydrogen atom and its bonding Si atom may also help identify the defect. We point out that if an E-center-like EPR signal is observed in the hydrogenated silicon sample while the correlation of the signal to the E center is hard to be established, one should consider if the signal can be assigned to the VH defect.

C. Dihydrogen-vacancy (VH_2) complex

In the VH_2 defect, the two silicon dangling bonds are saturated by the hydrogen impurity atoms. In the atomic

TABLE II. Calculated spin-unpaired electron energy levels and hyperfine-interaction parameters, arising from the paramagnetic spin of the wave function of the gap state, and wave-function coefficients for the atoms in the central cell of the neutral VH defect in silicon after two assumed Jahn-Teller distortions, labeled I and II. The energies of the levels are measured relative to the top of the valence band. Δx, Δy, and Δz are displacements of the atoms from their C_{3v} symmetric positions shown in Fig. 1(a). l, m, and n are the direction cosines of the axially symmetric axis of the hyperfine tensor at each atomic site, and θ is the angle between the direction of the axially symmetric axis and the $\langle 110 \rangle$ direction. The level localization is defined as the sum of the localizations η_j^2 of the defect states on all atoms in the defect central cell.

Case number	Energy level (eV)	Atomic site	Δx (Å)	Δy (Å)	Δz (Å)	a_j (10^{-6} eV)	b_j (10^{-6} eV)	θ (deg)	l	m	n	α_j^2	β_j^2	η_j^2	Level localization
I	0.72	H	0.052	0.052	−0.104	0.001						1.00		0.000	0.63
		Si_1	0.000	0.000	0.000	0.0001	0.0002	69.44	0.25	0.25	0.94	0.02	0.98	0.000	
		Si_2	−0.136	−0.136	0.000	1.892	0.180	144.73	−0.58	−0.58	0.58	0.21	0.79	0.501	
		Si_3	0.136	−0.136	0.000	0.228	0.023		0.60	−0.58	0.56	0.20	0.80	0.064	
		Si_4	−0.136	0.136	0.000	0.228	0.023		−0.58	0.60	0.56	0.20	0.80	0.064	
II	0.61	H	0.104	0.104	−0.208	0.002						1.00		0.000	0.62
		Si_1	0.000	0.000	0.000	0.0008	0.0005	60.55	0.35	0.35	0.87	0.04	0.96	0.001	
		Si_2	−0.272	−0.272	0.000	1.920	0.195	144.55	−0.58	−0.58	0.58	0.20	0.80	0.536	
		Si_3	0.272	−0.272	0.000	0.139	0.016		0.58	−0.59	0.56	0.18	0.82	0.042	
		Si_4	−0.272	0.272	0.000	0.139	0.016		−0.59	0.58	0.56	0.18	0.82	0.042	

TABLE III. Character table for the point symmetry group C_{2v}.

	E	C_2	σ_v	$\sigma_{v'}$
a_1	1	1	1	1
a_2	1	1	−1	−1
b_1	1	−1	1	−1
b_2	1	−1	−1	1

configuration shown in Fig. 1(b), the Hamiltonian of the defect is invariant under the operations of the point symmetry group C_{2v}. In order to specify unambiguously the labels for the irreducible representations in the group C_{2v} used in the present paper, we give in Table III its character table. In this table, σ_v is the reflection operation with respect to the mirror plane v containing the two hydrogen atoms, while $\sigma_{v'}$ is the reflection operation with respect to the mirror plane v' containing the two nonhydrogenated silicon atoms. Since the group C_{2v} can only have one-dimensional irreducible representations, no Jahn-Teller distortion can occur for the $V\mathrm{H}_2$ defect.

In Fig. 7 we display the calculated ΔLDOS's for the defect at the neutral ground state [denoted by $(V\mathrm{H}_2)^0$], corresponding to all the atomic sites in the central cell of the defect. Only the results of a_1, b_1, and b_2 symmetries are shown in this figure. For a_2 symmetry, no significant change in the LDOS is found for the $V\mathrm{H}_2$ defect. In Fig. 7, five localized defect states can be clearly identified: Associated with a_1 symmetry are two bound states at $E_v+0.05$ eV and $E_v-12.87$ eV and one resonance state at $E_v+5.10$ eV. Associated with b_1 and b_2 symmetries are one (resonance) state at an energy well above the lowest conduction band and one bound state at $E_v+0.72$ eV, respectively. In Table IV we only list the calculated energy positions of the two gap states for $(V\mathrm{H}_2)^0$. We have also done the calculations for the defect at the ground states of the single-positive and the single-negative charge states [denoted by $(V\mathrm{H}_2)^{1+}$ and $(V\mathrm{H}_2)^{1-}$, respectively] and at the neutral excited state [denoted by $(V\mathrm{H}_2)^{0*}$]. The reason for doing these will become clear when we compare our calculations with experiments. In these calculations, electronic structures are found to be very similar to $(V\mathrm{H}_2)^0$. Again, only the calculated results for the gap states of $(V\mathrm{H}_2)^{1+}$, $(V\mathrm{H}_2)^{1-}$, and $(V\mathrm{H}_2)^{0*}$ have been listed in Table IV.

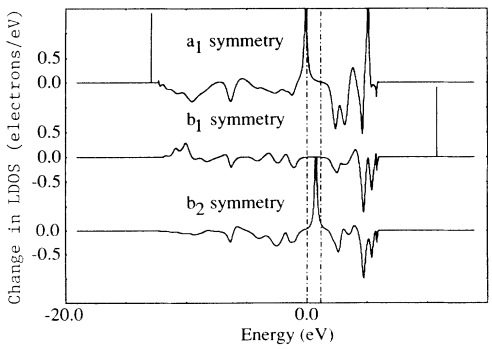

FIG. 7. Calculated changes in the local densities of states (ΔLDOS) of a_1, b_1, and b_2 symmetries induced by the neutral $V\mathrm{H}_2$ defect (in C_{2v} symmetry) in crystalline silicon, corresponding to all the atomic sites in the central cell of the defect. Units are electrons per eV. The spin degeneracy is excluded. The energy at the top of the valence band is set to zero. The edges of the fundamental band gap are identified by dot-dashed lines.

It seems that the electronic structure of the $V\mathrm{H}_2$ defect is more complicated than the $V\mathrm{H}$ defect. However, the calculations for the localization characters of the defect states will still help us understand it. We have found that for the defect in each of the four concerned defect states, the two bound states (one a_1 and one b_2 state) in the fundamental band gap are mainly localized on the two silicon atoms with nonhydrogen-saturated dangling bonds, whereas the other three defect states are localized on the other two silicon atoms and the two hydrogen atoms in the central cell of the defect. In Table IV the calculated localization characters of the two fundamental gap states are given. Based on these results, the one-electron molecular-orbital model of the $V\mathrm{H}_2$ defect can be constructed. This is shown in Fig. 8. The hybrids of the Si_1 and Si_2 atoms can be symmetrized to give an a_1 and a b_1 combination [Fig. 8(a)]. The same goes for the two hydrogen s orbitals [Fig. 8(c)]. The two a_1 (b_1) combinations (one from the two silicon hybrids and one from the two hydrogen s orbitals) will interact strongly, resulting in a bonding and an antibonding a_1 (b_1) state [Fig. 8(b)]. The two Si-H bonds are then formed as the two bonding

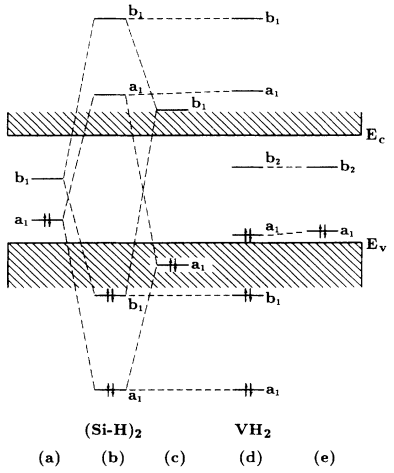

FIG. 8. Schematic illustration of the one-electron molecular-orbital treatment for the electronic structure of the ground state of the neutral $V\mathrm{H}_2$ defect (in C_{2v} symmetry) in crystalline silicon. (a) shows an a_1 and a b_1 energy level associated with the two hydrogen-saturated silicon hybrids towards the vacancy center. (c) shows an a_1 and a b_1 energy level associated with the two hydrogen s orbitals. (b) is the energy-level scheme resulting from interactions of the two a_1 states and the two b_1 states shown in (a) and (c). (e) shows an a_1 and a b_2 energy level formed from the two silicon dangling orbitals of the defect. (d) shows the electronic structure for the $V\mathrm{H}_2$ defect, obtained simply by the combination of the energy-level schemes given in (b) and (e). The two Si-H bonds are formed as four electrons are accommodated in the bonding a_1 and b_1 states formed from the hydrogen s orbitals and the hydrogen-saturated silicon hybrids.

TABLE IV. Calculated energy levels in the fundamental band gap and their localization characters α_j, β_j, and η_j for the $V\mathrm{H}_2$ defect in silicon. The energies of the levels are measured relative to the top of the valence band. The point symmetry group of the defect is C_{2v}. The sum on j in column 8 runs over the equivalent atoms only. The level localization is defined as the sum of the localizations of a defect state on all atoms in the central cell of the defect. The column labeled level occupancy indicates electron occupation of the gap levels at different states of the defect.

Defect state	Energy level (eV)	Symmetry	Atomic site	Number of equivalent sites	α_j^2	β_j^2	$\sum_j \eta_j^2$	Level localization	Level occupancy
$(V\mathrm{H}_2)^0$	0.05	a_1	H	2	1.00		0.005	0.38	2
			Si_1	2	0.14	0.86	0.009		
			Si_3	2	0.15	0.85	0.366		
	0.72	b_2	Si_1	2		1.00	0.006	0.66	0
			Si_3	2	0.20	0.80	0.650		
$(V\mathrm{H}_2)^{1+}$	0.02	a_1	H	2	1.00		0.003	0.17	1
			Si_1	2	0.09	0.91	0.004		
			Si_3	2	0.14	0.86	0.160		
	0.64	b_2	Si_1	2		1.00	0.000	0.65	0
			Si_3	2	0.20	0.80	0.654		
$(V\mathrm{H}_2)^{1-}$	0.29	a_1	H	2	1.00		0.005	0.60	2
			Si_1	2	0.26	0.74	0.013		
			Si_3	2	0.17	0.83	0.579		
	1.00	b_2	Si_1	2		1.00	0.000	0.57	1
			Si_3	2	0.25	0.75	0.574		
$(V\mathrm{H}_2)^{0*}$	0.12	a_1	H	2	1.00		0.006	0.48	1
			Si_1	2	0.18	0.82	0.011		
			Si_3	2	0.15	0.85	0.476		
	0.79	b_2	Si_1	2		1.00	0.000	0.64	1
			Si_3	2	0.22	0.78	0.636		

states are occupied by the four electrons. Since the b_1 bonding state resembles well the corresponding Si-Si bond in the crystal, it will contribute the valence band in a wide range of energies. Therefore, no localized b_1 defect state has been found in the valence band. The remaining silicon dangling bonds, on the other hand, can be symmetrized to give an a_1 and a b_2 state [Fig. 8(e)]. We note here that the energy separation between the a_1 and b_2 states of the silicon dangling orbitals has reasonably been set larger than the energy separation between the a_1 and b_1 states of the two silicon hybrids saturated by the hydrogen atoms, since the interaction between the former two states behaves as the first-nearest-neighbor interactions, while that between the latter two states behaves as the second-nearest-neighbor interactions. We note also that the b_2 state is located, as it should be, almost at the same energy as the t_2 gap state of the isolated ideal silicon vacancy. The electronic structure of the $V\mathrm{H}_2$ defect [Fig. 8(d)] are simply obtained by combining the symmetric states of the two hydrogen s orbitals and the two hydrogen-saturated silicon hybrids [Fig. 8(b)] and the symmetric states of the two silicon dangling bonds [Fig. 8(e)]. The interactions between the a_1 states can occur. However, these interactions must be very weak, due to the large energy separations between these states. Our results clearly show that the ground state $(V\mathrm{H}_2)^0$ of the neutral defect is a spin-singlet state, consistent with the experimental work of Ref. 12.

Experimentally, the $V\mathrm{H}_2$ complex defect has been studied with the use of the DLTS and ODMR techniques. In the study by DLTS,[13] an electron trap was observed in n-type silicon and was assigned to the $V\mathrm{H}_2$ defect with no charge state of the defect being conclusively determined. The activation energy of the electron trap was determined to be 0.2 eV. We have found that the $(V\mathrm{H}_2)^{1-}$ defect has a single-particle gap state, occupied by one electron, at $E_c-0.14$ eV. This result strongly supports that the electron trap observed in the DLTS experiment is associated with the defect at the single-negative charge state $(V\mathrm{H}_2)^{1-}$.

In the study by ODMR,[12] a spin triplet was identified to be $(V\mathrm{H}_2)^{0*}$, the excited state of the $V\mathrm{H}_2$ defect at its neutral charge state. The model proposed for understanding the experimental results is based on the requirements that the $V\mathrm{H}_2$ defect introduce two energy levels in the fundamental band gap and the defect can stay at the

$(VH_2)^{1-}$ [or $(VH_2)^{1+}$] charge state. Our calculations clearly support the proposed model. In addition, the authors of this study have calculated the localizations of the electronic wave function of the spin-triplet state from the measured hyperfine-interaction tensors. The general agreement between the experimental results and our calculated results is also achieved. We have to note that for the spin-triplet electronic state, a linear combination of the products of the one-electron wave functions of the two gap states should, to the lowest-order approximation, be used in the calculations of the hyperfine-interaction tensors.[44] When the lobes of the p function on an atomic site in the one-electron wave functions of the two gap states have the same symmetry axis directions, calculations by using one-electron wave functions will give the same results as the calculations by using the full triplet electron wave functions, i.e., the linear combinations of the products of the one-electron wave functions of the two gap states. In the present paper, the calculations for the spin-triplet state of $(VH_2)^{0*}$ are done by using the full triplet wave functions. The results of our calculations are given in Table V. Deviations from axial symmetry in the hyperfine-interaction tensors at the silicon sites in the central cell of the defect have been found. To describe, in general, these hyperfine tensors, we have to use three parameters, a_j, b_j, and c_j. In terms of these, the largest principal value A_1 of the hyperfine tensor $\overleftrightarrow{A}$ is given by $A_1=a_j+2b_j$, the second largest one A_2 by $A_2=a_j-b_j+c_j$, and the smallest one A_3 by $A_3=a_j-b_j-c_j$. As can be seen in Table V, the deviations from the axial symmetry in the hyperfine tensors at the silicon sites are all negligibly small. For the Si_3 site, the direction of the approximate symmetry axis is in the mirror plane v' containing the two nonhydrogenated silicon atoms and very close to the $\langle 1\bar{1}1\rangle$ direction, which is the axial direction of the hyperfine tensor assumed in the ODMR study. For the isotropic component of the hyperfine tensor at the Si_3 site, our predictions are somehow larger than that derived from the ODMR study. This results from our having predicted a larger value for the s character of the one-electron wave functions of the two gap states than the ODMR study.

The calculations for the hyperfine-interaction parameters arising from the paramagnetic spin of the wave function of the unpaired electron in the gap state have also been carried out for the spin-doublet state $(VH_2)^{1-}$. The results are also presented in Table V. If the silicon sample is prepared under the same condition as described in Ref. 13, it is one can expect to observe an EPR signal arising from $(VH_2)^{1-}$. Thus our calculations may help to identify it.

D. Trihydrogen-vacancy (VH_3) complex

In the atomic configuration shown in Fig. 1(c), the Hamiltonian of the VH_3 defect is invariant under the operations of the point symmetry group C_{3v}. In Fig. 9 we display the calculated ΔLDOS's of a_1 and e symmetries for the defect at the neutral state, corresponding to all the atomic sites in the central cell of the defect. No significant changes in the LDOS of a_2 symmetry are found. As can be seen in this figure, three localized states appear due to the VH_3 defect. For the a_1 symmetry, the defect introduces a defect state at $E_v-15.86$ eV, well below the calculated valence band, and a bound state at $E_v+0.40$ eV, in the fundamental band gap. For the e symmetry, the defect introduces a (resonance) state at $E_v+10.71$ eV, well above the lowest conduction band. We have found that the two defect states far away from the fundamental band gap are essentially localized on the hydrogen and their bonding atoms, while the bound state in the fundamental band gap is basically localized on the Si_1 atom, whose dangling orbital has not been saturated by a hydrogen atom. The results of our calculations for the fundamental gap state are given in Table VI.

The results of our calculations can still be easily understood with the use of the one-electron molecular-orbital model shown in Fig. 10. The three silicon hybrids of the Si_2, Si_3, and Si_4 atoms towards the vacancy center [Fig. 10(a)] interact strongly with the three hydrogen s orbitals

TABLE V. Calculated hyperfine-interaction parameters, arising from the wave functions of the spin-unpaired electrons in the gap state, of the VH_2 defect in the spin-triplet state ($S=1$) $(VH_2)^{0*}$ and the spin-doublet state ($S=\frac{1}{2}$) $(VH_2)^{1-}$ in silicon for the atoms in the central cell of the defect. For $(VH_2)^{0*}$, l, m, and n are defined as the direction cosines of the first principal axis of the hyperfine tensor, on which the hyperfine tensor has the largest principal value, and θ is the angle between the direction of the first principal axis of the hyperfine tensor and the $\langle 110\rangle$ direction for Si_1 or the $\langle 1\bar{1}0\rangle$ direction for Si_3. For $(VH_2)^{1-}$, l, m, n, and θ are the corresponding values for the symmetry axis of the hyperfine tensor. The numbers in the brackets are ODMR values derived from Ref. 12.

Defect state	Total spin S	Atomic site	a_j (10^{-6} eV)	b_j (10^{-6} eV)	c_j (10^{-9} eV)	θ (deg)	l	m	n
$(VH_2)^{0*}$	1	H	0.008 (0.024)						
		Si_1	0.009	0.001	0.004	57.40	0.381	0.381	0.842
		Si_3	0.965 (0.620)	0.102 (0.150)	0.175 (0.000)	36.91 (35.26)	0.565 (0.577)	−0.565 (−0.577)	0.601 (0.577)
$(VH_2)^{1-}$	$\frac{1}{2}$	Si_1		0.004		90.00	0.707	−0.707	0.000
		Si_3	1.278	0.098		36.11	0.571	−0.571	0.589

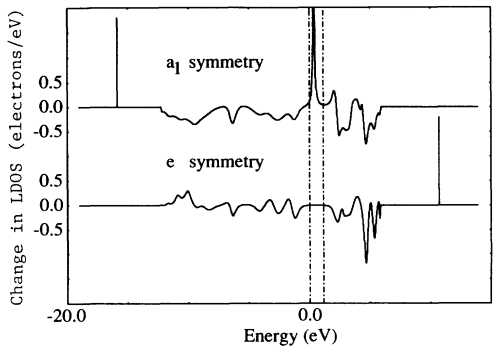

FIG. 9. Calculated changes in the local densities of states (ΔLDOS) of a_1 and e symmetries induced by the neutral $V\mathrm{H}_3$ defect (in C_{3v} symmetry) in crystalline silicon, corresponding to all the atomic sites in the central cell of the defect. Units are electrons per eV. The spin degeneracy is excluded. The energy at the top of the valence band is set to zero. The edges of the fundamental band gap are identified by dot-dashed lines.

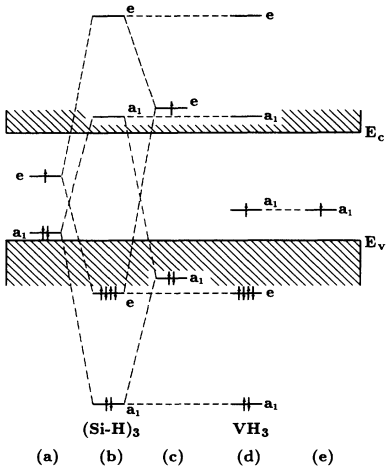

FIG. 10. Schematic illustration of the one-electron molecular-orbital treatment for the electronic structure of the neutral $V\mathrm{H}_3$ defect (in C_{3v} symmetry) in crystalline silicon. (a) shows an a_1 and an e energy level associated with the three hydrogen-saturated silicon hybrids towards the vacancy center. (c) shows an a_1 and an e energy level associated with the three hydrogen s orbitals. (b) is the energy-level scheme resulting from interactions between the two a_1 states and between the two e states shown in (a) and (c). (e) shows an a_1 level due to the only silicon dangling orbital of the defect. (d) shows the electronic structure for the $V\mathrm{H}_3$ defect, obtained simply by the combination of the energy-level schemes given in (b) and (e). The three Si-H bonds are formed as six electrons are accommodated in the a_1 and e bonding states associated with the three hydrogen s orbitals and the three hydrogen-saturated silicon hybrids.

[Fig. 10(c)], giving a pair of a_1 states and a pair of e states [Fig. 10(b)]. The six electrons brought by the three silicon hybrids and the three hydrogen s orbitals occupy the bonding a_1 and e states as shown in Fig. 10(b), resulting in the formation of the three Si-H bonds in the defect. However, our calculations show that no localized states associated with the three Si-H atomic pairs appear in the calculated valence and conduction bands (see Fig. 9). This clearly indicates that both the Si-H bonding e state and the Si-H antibonding a_1 state resemble the corresponding Si-Si bonding and antibonding states in the crystal very well. Figure 10(e) shows an a_1 state associated with the remaining silicon dangling orbital for the $V\mathrm{H}_3$ defect. The global electronic structure of the $V\mathrm{H}_3$ defect is given in Fig. 10(d). Only very weak interactions between the a_1 state associated with the silicon atom with the dangling bond and the a_1 states associated with the three Si-H atomic pairs are found (see Table VI). The symmetry-conserved lattice distortions can occur. Our model, however, predicts that the lattice distortions will not affect the properties, such as energy position and localization, of the fundamental gap state significantly, since this state is basically a single silicon-dangling-bond state.

We predict that for the $V\mathrm{H}_3$ defect at the neutral state, the a_1 gap level is occupied by one spin-unpaired electron, leading to a paramagnetic spin-doublet state. In order to help experimentalists to identify the defect, we present in Table VII the calculated hyperfine-interaction parameters, arising from the paramagnetic spin of the wave function of the unpaired electron in the gap state, of the neutral $V\mathrm{H}_3$ defect for the atoms in the central cell of the defect. As can be seen in this table, very large hyperfine interactions will arise from the Si_1 atom, and the axially symmetric axis of the corresponding hyperfine tensor will be along the $\langle 111 \rangle$ direction.

TABLE VI. A calculated energy level in the fundamental band gap and its localization characters α_j, β_j, and η_j for the neutral $V\mathrm{H}_3$ defect in silicon. The energy of the level is measured relative to the top of the valence band. The point symmetry group of the defect is C_{3v}. The sum on j in column 7 runs over the equivalent atoms only. The level localization is defined as the sum of the localizations of the defect state on all atoms in the central cell of the defect. The level occupancy is electron occupation of the gap level of the neutral defect.

Energy level (eV)	Symmetry	Atomic site	Number of equivalent sites	α_j^2	β_j^2	$\sum_j \eta_j^2$	Level localization	Level occupancy
0.40	a_1	H	3	1.00		0.004	0.63	1
		Si_1	1	0.18	0.82	0.625		
		Si_2	3	0.43	0.57	0.003		

TABLE VII. Calculated hyperfine-interaction parameters, arising from the paramagnetic spin of the wave function of the gap state, of the neutral $V\mathrm{H}_3$ defect in silicon for the atoms in the central cell of the defect. l, m, and n are the direction cosines of the axially symmetric axis of the hyperfine tensor at each atomic site, and θ is the angle between the direction of the axially symmetric axis and the $\langle 110 \rangle$ direction.

Atomic site	a_j (10^{-6} eV)	b_j (10^{-6} eV)	θ (deg)	l	m	n
H	0.008					
Si_1	2.058	0.232	35.26	0.577	0.577	0.577
Si_2	0.007	0.000	172.32	−0.704	−0.704	0.095

V. SUMMARY AND CONCLUSIONS

In this paper we have reported on self-consistent tight-binding calculations for the electronic structure of the four hydrogen-vacancy complexes, namely, $V\mathrm{H}$, $V\mathrm{H}_2$, $V\mathrm{H}_3$, and $V\mathrm{H}_4$, in crystalline silicon. The calculations were done with the use of the recursion method and the large repeated supercell approximation. Using a new numerical method, the wave functions of the gap states of the complex defects were calculated. The hyperfine-interaction parameters arising from the paramagnetic spin of the unpaired electron in the gap state of the defects were, in turn, derived from the calculated wave functions. The effect of the symmetry-conserved lattice distortions of hydrogen atoms on the electronic structure was particularly studied for the $V\mathrm{H}_4$ defect. The results can be used to assess the validity of the atomic structures which we have proposed for the four hydrogen-vacancy complexes in Fig. 1. We have also proposed a set of one-electron molecular-orbital models for the four defects. All the electronic structures of the defects can be well understood with our models.

In the $V\mathrm{H}_4$ complex defect, the electrical activity of the isolated silicon vacancy is found to be well passivated by the four hydrogen atoms bonding to the neighboring silicon atoms of the vacancy in agreement with early theoretical studies. The crucial input parameter in our calculations for $V\mathrm{H}_4$ is the Si-H bond length or, equivalently, the distance (d) of the hydrogen atoms from the vacancy center. We have found that using the method described in this paper, a good choice of the parameter is $d=0.90$ Å, which gives a reasonable Si-H bond length of $d=1.45$ Å and has been used in the calculations for the other three hydrogen-vacancy complexes in the cases where no lattice distortion is considered. We have found that the t_2 gap state of the isolated vacancy has been pushed down to the valence band, while the a_1 resonance state of the isolated vacancy at the top of the valence band has been pushed up to the conduction band. We have also found that when the hydrogen atoms are moved away from their bonding silicon atoms, an unoccupied a_1 level will fall into the band gap from the conduction band. All these calculated results indicate that the strong interactions of hydrogen s orbitals with silicon hybrids are responsible for the passivation of the vacancy defects in silicon.

In the $V\mathrm{H}$, $V\mathrm{H}_2$, and $V\mathrm{H}_3$ complex defects, the electrical activities of the isolated silicon vacancy are all only partially passivated by hydrogen atoms. For the $V\mathrm{H}$ defect in its C_{3v} point symmetry configuration shown in Fig. 1(a), an a_1 strong resonance state at the top of the valence band and an e bound state in the fundamental band gap were found. We have demonstrated that the two defect states are mainly silicon-dangling-bond-like and have almost no contributions from the hydrogen atoms and the hydrogen-saturated silicon atoms. For instance, for the e gap state at $E_v+0.72$ eV, about 60% (0.0%) of its wave function is localized on the three Si atoms having dangling bonds (the H and its bonding Si atoms). We have shown that the hydrogen s orbitals and the hydrogen-saturated silicon hybrids can only give the defect states at energies far from the fundamental band gap. We have predicted that the $V\mathrm{H}$ defect in its neutral charge state should undergo a Jahn-Teller distortion since the e gap state is occupied by only one spin-unpaired electron. The Jahn-Teller distortion will lower the symmetry of the defect from C_{3v} to C_{1h} and, thus, cause a splitting of the e gap level according to $e=a'+a''$ with a spin-unpaired electron at the a' gap state. We have found that over 50% of the wave function of the spin-unpaired electron is accounted for on one of the three nonhydrogenated Si atoms surrounding the vacancy. The EPR spectra of the $V\mathrm{H}$ defect are predicted to be very similar to the Si E center, revealing a difficulty in its identification. A clue to the identification of the defect is the Si-H bond, which should have a contribution to the infrared-absorption spectra. In addition, small but not vanishing hyperfine interactions with the hydrogen and its bonding Si atoms are predicted for the defect. This prediction may also help identify it.

The $V\mathrm{H}_2$ defect in the configuration as shown in Fig. 1(b) has the C_{2v} point group symmetry and thus does not undergo any Jahn-Teller distortions. We have found that the defect introduces an a_1 and a b_2 state into the fundamental band gap. As we have shown for the $V\mathrm{H}$ defect, both of the two gap states of the $V\mathrm{H}_2$ defect are silicon-dangling-bond-like. The two hydrogen s orbitals and two hydrogen-saturated silicon hybrids have only very small contributions to the two gap states and can only create localized defect states at energies far from the band gap. Four defect states of $V\mathrm{H}_2$ have been studied. They are the ground states of the two charge defect states [$(V\mathrm{H}_2)^{1+}$ and $(V\mathrm{H}_2)^{1-}$] and the ground and lowest excited states of the neutral defect state [$(V\mathrm{H}_2)^{0}$ and $(V\mathrm{H}_2)^{0*}$]. We predict that the b_2 gap state in the $(V\mathrm{H}_2)^{1-}$ defect stays at $E_c-0.14$ eV and occupied by

one electron, which supports the assignment of the Z center to the defect in a DLTS study.[13] In the defect state $(VH_2)^0$, the two electrons are found to be accommodated in the a_1 gap state with their spins paired off, giving rise to an EPR inactive defect center. However, the neutral excited state $(VH_2)^{0*}$ of the defect is expected to be paramagnetic, since the two electrons with parallel spins can be accommodated in the a_1 and the b_2 gap states, respectively, leading to a spin-triplet electron state. The calculated hyperfine-interaction parameters for the neutral excited state $(VH_2)^{0*}$ of the defect agree in general with the ODMR study of Ref. 12, although we have only done calculations for the hyperfine-interaction parameters arising from the wave functions of gap states alone. However, with the use of the zeroth-order spin-triplet electronic wave functions, we predict that the hyperfine-interaction tensors at the silicon atomic sites surrounding the vacancy are not axially symmetric, but the deviations from the axial symmetries are very small. We also predict that the largest principal axes of the hyperfine tensors are slightly oriented from the tetrahedral bonding directions of the corresponding silicon atoms. In addition, we have also derived the hyperfine-interaction parameters arising from the paramagnetic spin of the wave function of the gap state for the $(VH_2)^{1-}$ defect. The results should be useful for confirming the assignment of the defect in the DLTS study of Ref. 13 and for further characterizing the defect.

The remaining hydrogen-vacancy complex studied in this paper is VH_3. The defect has the C_{3v} point group symmetry and a relatively simple electronic structure. We predicted that the defect can only introduce an a_1 state into the fundamental gap and, thus, no Jahn-Teller distortion can occur for the defect. We have shown that the gap state is silicon-dangling-bond-like and about 60% of its wave function is localized on the only dangling orbital of the defect. The atomic orbitals associated with the three Si-H atomic pairs of the defect make nearly zero contributions to the gap state. Accordingly, a strong hyperfine interaction at the nonhydrogen-saturated neighboring silicon nucleus of the defect is predicted.

We have thus been able to predict a number of important features for the electronic structure of the hydrogen-vacancy complexes in silicon. The primary conclusions of this study are as follows. A silicon dangling bond can be well passivated by a hydrogen atom, whether or not there are any other silicon dangling bonds or Si-H atomic pairs in the vacancy region. The remaining electrical activity of the defects can all simply be accounted for by the nonhydrogenated silicon dangling bonds. In a forthcoming paper[45] we will show that if the nonhydrogenated silicon atoms in the defects are all replaced by phosphorus atoms, which results in the hydrogen-phosphorus-vacancy complex defects, all the electrically active states will be removed from the fundamental band gap. It is hoped that the results of this theoretical study can be used as a guideline for further investigations of the hydrogen-vacancy-related defects in silicon.

ACKNOWLEDGMENTS

The author is grateful to Professor L. Hedin for his kind support and continuous encouragement and for his constructive remarks on the manuscript.

APPENDIX

In the calculations for the defects involving interstitial impurities in semiconductors, the basis set of the host crystal in the tight-binding approximation needs to be augmented by introducing the localized orbitals centered on the interstitial sites, in order to describe the perturbation potential due to the impurities effectively. This is just the reverse of the usual procedure in the calculations for vacancies in semiconductors (see, for instance, Ref. 46). Thus, in the calculations for, for instance, an impurity in a semiconductor, the Hamiltonian of the host crystal plus the interstitial in a localized orbital basis is given by

$$H=\begin{bmatrix} H^0 & W \\ W^\dagger & H^I \end{bmatrix}, \tag{A1}$$

where H^0 consists of the tight-binding parameters of the host atoms, H^I consists of only the tight-binding parameters of the interstitial atom, and W is the matrix that couples the interstitial atom with the host atoms. In an sp^3 basis, H^0 is an $8N\times 8N$ square matrix, where N is the number of unit cells, while H^I is a diagonal 4×4 matrix. In our approach, the diagonal elements of H^0 and H^I will be calculated self-consistently in the procedure described in Sec. III C. The off-diagonal elements of H^0 and the elements of W are taken to be the corresponding elements of the tight-binding Hamiltonian of the perfect crystal, scaled with distance and orbital energies according to the Wolfsberg-Helmholz formula [see Eq. (3) in Sec. III B]. We believe that the Wolfsberg-Helmholz formula should be more appropriate for the calculations for the defects involving interstitial impurities than Harrison's d^{-2} rule (where d is the distance between two atoms),[47] because Harrison's d^{-2} rule was derived for the equilibrium separations in crystals and should work mainly for the atoms in the neighborhood of the corresponding equilibrium positions.[48]

[1]S. J. Paerton, J. W. Corbett, and T. S. Shi, Appl. Phys. A **43**, 153 (1987).

[2]E. E. Haller, in *Proceedings of the 20th International Conference on the Physics of Semiconductors*, edited by E. M. Anastassakis and J. D. Joannopoulos (World Scientific, Singapore, 1990), Vol. 1, p. 29.

[3]K. Bergman, M. Stavola, S. J. Pearton, and T. Hayes, Phys. Rev. B **38**, 9643 (1988).

[4]A. A. Bonapasta, A. Lapiccirella, N. Tomassini, and M. Capizzi, Phys. Rev. B **36**, 6228 (1987).

[5]K. J. Chang and D. J. Chadi, Phys. Rev. Lett. **60**, 1422 (1988).
[6]P. J. H. Denteneer, C. G. Van der Walle, and S. Pantelides, Phys. Rev. B **39**, 10 809 (1989); Phys. Rev. Lett. **62**, 1884 (1989).
[7]S. K. Estreicher, L. Throckmorton, and D. S. Marynick, Phys. Rev. B **39**, 13 241 (1989).
[8]N. M. Johnson, C. Herring, and D. J. Chadi, Phys. Rev. Lett. **56**, 769 (1986).
[9]S. B. Zhang and D. J. Chadi, Phys. Rev. B **41**, 3882 (1990).
[10]P. J. H. Denteneer, C. G. Van der Walle, and S. Pantelides, Phys. Rev. B **41**, 3885 (1990).
[11]G. G. Deleo, W. B. Fowller, T. M. Sudol, and K. J. O'Brien, Phys. Rev. B **41**, 7581 (1990).
[12]W. M. Chen, O. O. Awadelkarim, B. Monemar, J. L. Lindström, and G. S. Oehrlein, Phys. Rev. Lett. **64**, 3042 (1990).
[13]Du Yong-Chang, Zhang Yu-Feng, Qin Guo-Gang, and Meng Xiang-Ti, Chin. J. Phys. **5**, 21 (1985) [Acta Phys. Sin. **33**, 477 (1984)].
[14]B. B. Nielsen, J. Olajos, and H. G. Grimmeiss, Phys. Rev. B **39**, 3330 (1989).
[15]V. A. Singh, C. Weigel, J. W. Corbett, and L. M. Roth, Phys. Status Solidi B **81**, 637 (1977).
[16]W. E. Pickett, Phys. Rev. B **23**, 6603 (1981).
[17]G. G. Deleo, W. B. Fowller, and G. D. Watkins, Phys. Rev. B **29**, 1819 (1984).
[18]M. Wolfsberg and L. Helmholz, J. Chem. Phys. **20**, 837 (1952).
[19]O. F. Sankey and J. D. Dow, Phys. Rev. B **27**, 7641 (1983).
[20]J. van der Rest and P. Pecheur, J. Phys. Chem. Solids B **45**, 563 (1984).
[21]U. Lindefelt and A. Zunger, Phys. Rev. B **26**, 846 (1982); U. Lindefelt, J. Phys. C **11**, 3651 (1978).
[22]R. Haydock, in *The Recursion Method and Its Applications,* edited by D. G. Pettifor and D. L. Weaire, Springer Series in Solid-State Science Vol. 58 (Springer-Verlag, Berlin, 1985), p. 8.
[23]R. Haydock, V. Heine, and M. J. Kelly, J. Phys. C **5**, 2845 (1972); **8**, 2591 (1975).
[24]R. Haydock, in *Solid State Physics,* edited by H. Ehrenreich, F. Seitz, and D. Turnbull (Academic, New York, 1980), Vol. 35, p. 215.
[25]C. M. M. Nex, J. Phys. A **11**, 653 (1978); in *The Recursion Method and Its Applications* (Ref. 22), p. 52.
[26]Hongqi Xu, J. Phys. A **24**, L765 (1991).
[27]P. Pecheur, G. Toussaint, and M. Lannoo, in *Defects and Radiation Effects in Semiconductors,* edited by R.R. Hasiguti (Institute of Physics and Physical Society, Bristol, London, 1981), p. 147.
[28]P. Pecheur and G. Toussaint, in *Defects in Semiconductors* (Materials Science Forum Vols. 10–12), edited by H. J. von Bardeleben (Trans Tech, Aedermannsdorf, Switzerland, 1986), p. 43.
[29]Hongqi Xu and U. Lindefelt, Int. J. Mod. Phys. B **3**, 863 (1989).
[30]P. Pecheur and G. Toussaint, Physica B **116**, 112 (1983).
[31]C. Delerue, G. Allan, and M. Lannoo, in *Defects in Semiconductors* (Ref. 28), p. 37.
[32]Hongqi Xu and U. Lindefelt, in *Impurities, Defects and Diffusion in Semiconductors: Bulk and Layered Structure,* edited by D. J. Wolford, J. Bernholc, and E. E. Haller (Materials Research Society, Pittsburgh, PA, 1990), p. 287.
[33]J. C. Slater and G. F. Koster, Phys. Rev. **94**, 1498 (1954).
[34]W. A. Harrison, Phys. Rev. B **23**, 5230 (1981).
[35]Hongqi Xu, Ph.D. thesis, University of Lund, 1991.
[36]Hongqi Xu and U. Lindefelt, Phys. Rev. B **41**, 5979 (1990).
[37]Hongqi Xu, J. Appl. Phys. **68**, 4077 (1990).
[38]H. Overhof, M. Scheffler, and C. M. Weinert, Phys. Rev. B **43**, 12 494 (1991).
[39]G. D. Watkins, in *Semiconductors and Molecular Crystals,* Vol. 2 of *Point Defects in Solids,* edited by J. H. Crawford, Jr. and L. M. Slifkin (Plenum, New York, 1975), p. 333.
[40]G. D. Watkins and J. W. Corbett, Phys. Rev. **121**, 1001 (1961).
[41]G. D. Watkins and J. W. Corbett, Phys. Rev. **134**, A1359 (1964).
[42]J. R. Morton and K. F. Preston, J. Mag. Reson. **30**, 577 (1978).
[43]A. Carrington and A. D. McLachlan, *Introduction to Magnetic Resonance* (Harper & Row, New York, 1967).
[44]N. M. Atherton, *Electron Spin Resonance: Theory and Applications* (Halsted, New York, 1973).
[45]Hongqi Xu (unpublished).
[46]J. Bernholc and S. T. Pantelides, Phys. Rev. B **18**, 1780 (1978).
[47]W. A. Harrison, *Electronic Structure and the Properties of Solids* (Freeman, San Francisco, 1980).
[48]S. Froyen and W. A. Harrison, Phys. Rev. B **20**, 2420 (1979).